IFM-GEOMAR REPORT

IFM-GEOMAR
Leibniz-Institut für Meereswissenschaften
an der Universität Kiel

FS Maria S. Merian
Fahrtbericht / Cruise Report MSM 04-2

Seismic Wide-Angle Profiles

Fort-de-France – Fort-de-France
03.01. - 19.01.2007

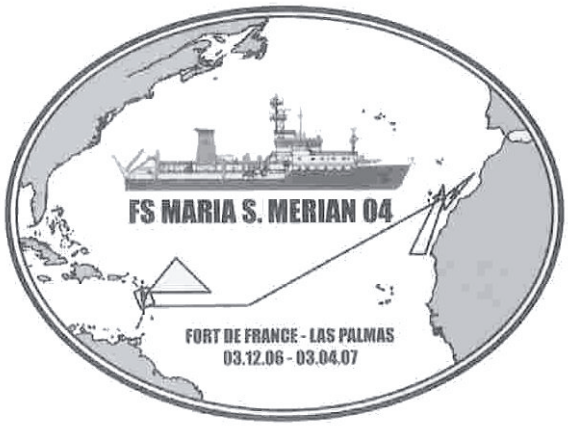

Berichte aus dem Leibniz-Institut
für Meereswissenschaften an der
Christian-Albrechts-Universität zu Kiel

Nr. 12
Juni 2007

IFM-GEOMAR
Leibniz-Institut für Meereswissenschaften
an der Universität Kiel

FS Maria S. Merian
Fahrtbericht / Cruise Report MSM 04-2

Seismic Wide-Angle Profiles

Fort-de-France – Fort-de-France
03.01. - 19.01.2007

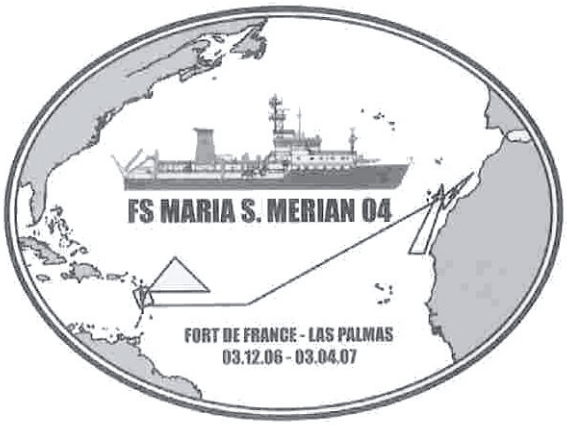

Berichte aus dem Leibniz-Institut
für Meereswissenschaften an der
Christian-Albrechts-Universität zu Kiel

Nr. 12, Juni 2007

ISSN Nr.: 1614-6298

IFM-GEOMAR
Leibniz-Institut für Meereswissenschaften
an der Universität Kiel

Das Leibniz-Institut für Meereswissenschaften ist ein Institut der Wissenschaftsgemeinschaft Gottfried Wilhelm Leibniz (WGL)

The Leibniz-Institute of Marine Sciences is a member of the Leibniz Association (Wissenschaftsgemeinschaft Gottfried Wilhelm Leibniz).

Herausgeber / Editor:
Ernst Flüh

IFM-GEOMAR Report
ISSN Nr.: 1614-6298

Leibniz-Institut für Meereswissenschaften / Leibniz-Institute of Marine Sciences
IFM-GEOMAR
Dienstgebäude Westufer / West Shore Building
Düsternbrooker Weg 20
D-24105 Kiel
Germany

Leibniz-Institut für Meereswissenschaften / Leibniz-Institute of Marine Sciences
IFM-GEOMAR
Dienstgebäude Ostufer / East Shore Building
Wischhofstr. 1-3
D-24148 Kiel
Germany

Tel.: ++49 431 600-0
Fax: ++49 431 600-2805
www.ifm-geomar.de

Contents

1 Introduction

The Hellenic Arc in Greece and the Lesser Antilles Island Arc that comprises French Departments are the two European active subduction zones prone for major Earthquakes. The major earthquake (EQ) and Tsunami catastrophe of the December 26, 2004 North-Sumatra-Andaman subduction zone recalls that even "quiet" subduction zones may have been wrongly considered as being mainly aseismic and unable to generate large EQ's and may indeed be the place of major telluric risk. More basically, 90% of the worldwide seismic energy release and 9/10 of the largest EQ's on record and the major tsunamis occur in subduction zones.

This project presents a scientific measurement approach for the detection of new types of seismic signals, as well as deep structural images that are relevant to the problem, being possible heralds of mega-thrust earthquakes. This will be applied in the Lesser Antilles Arc, that may be prone for M>8 EQ's as it shares characters of the Sumatra-Andaman case. These water-related phenomena, deep seismic tremor and silent EQ, were recently discovered in Japan and NW US subduction zones, where advanced technologies and methods have been applied. These transients are instead low-frequency signals of still unknown seismic activity, involving fluids and the ductile domain at depth. They were reported to have their source region close to the inter-plate subduction boundary, the mega-thrust fault plane, where possible water content has been revealed by deep structural seismic images. Importantly these transient signals are observed in advance of major M>8 EQ's expected there. They might in case be considered as possible silent heralds of mega-thrust EQ's and monitored. This scientific measurement approach, for detection of signs of place and time of major subduction EQ's may open the way to monitoring evolution, with high-yield/high-risk possible societal impact for hazard preparedness and mitigation.

Bathymetric mapping along the plate boundary is conducted where no previous data exists and along the forearc north of 17 $^\circ$ N and south of 14 $^\circ$ N. Existing high-resolution data is combined with the data acquired by FS Maria S. Merian to achieve full coverage of the plate margin. Bathymetric mapping of the forearc to the north and south of the seismic working area will as a first indicator unravel lateral changes in the structure of the forearc (e.g. variation in the frontal taper or changes in the compressional setting manifested in tectonic structures visible at the seafloor (i.e. folds and surface traces of faults)). These investigations are crucial to understand the entire margin segment, even in the absence of seismic investigations.

The main goal of the work using FS Maria S. Merian is the mapping of the location, size and spatial variation of the potentially seismogenic megathrust fault on the Antilles subduction boundary interplate. This will bring the Antilles subduction zone out of the unknown "white areas" on the map. It results from a dense network of approximately 50 ocean bottom instruments (OBH/OBS) to be deployed for a period of 4-6 months in conjunction with an onshore array. In addition, high-resolution mapping will yield information of the surface traces of potential fault zones and areas prone for submarine landslides. The multi-scale/multi-method work schedule (high-resolution multibeam bathymetry, reflection seismic imaging of the crustal portion of the margin, deep-penetrating wide angle seismic-profiling, earthquake monitoring) is essential for the complete comprehension of these new classes of seismic signals, which must be interpreted in the framework of morphological information, deep seismic imaging from active reflection/refraction seismics and seismology.

2 Geological settings of Lesser Antilles Arc

The Lesser Antilles arc is a ∼850 km long island arc formed by the subduction of the Atlantic seafloor under the Caribbean plate. The Caribbean plate is bounded to the north and to the south by two systems of strike-slip faults ([3], [47], [58], [64], [86], [70], [87], [136]); with a strongly curved subduction zone in between forming its eastern boundary (Fig. 2.1). This subduction zone absorbs the ENE motion between the American and the Caribbean plates, that converge at a rate of ∼2 cm/yr ([33], [34], [35]).

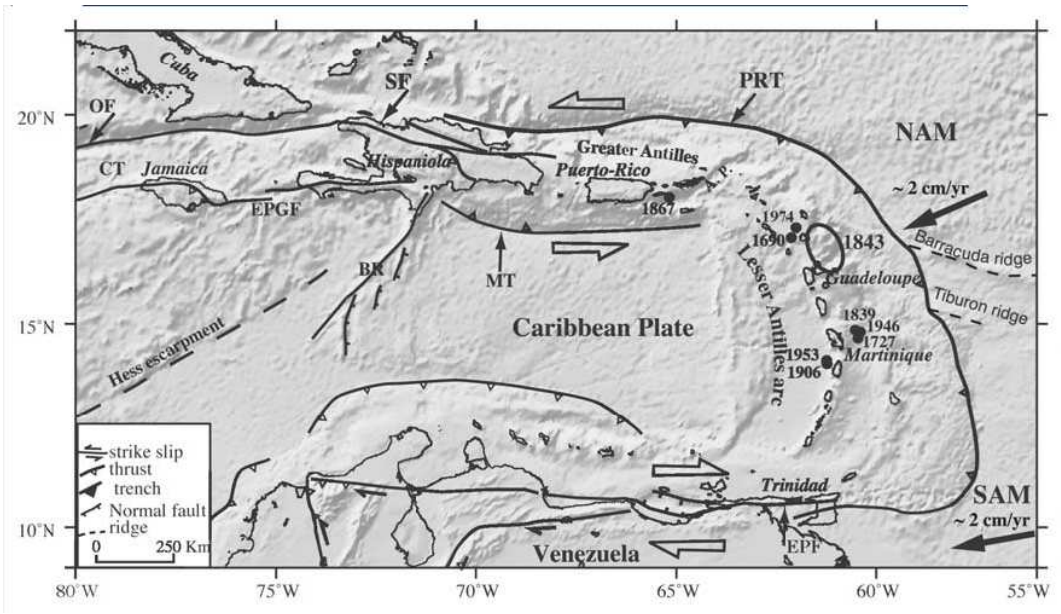

Fig. 2.1: Geodynamic setting of the Lesser Antilles arc [44]. Subduction rates from DeMets et al. [33] and Weber et al., 2001. CT: Cayman Trough, OF: Oriente Fault zone, EPGF: Enriquillo-Plantain Garden fault zone; BR: Beata Ridge; MT: Muertos trough, PRT: Puerto Rico trench, EPF: El Pilar Fault zone. Black circles: major historical earthquakes (I VIII-IX, M > 7) in the Lesser Antilles arc with dates after [13]; [43]; [104]. The patch ruptured by the 1843 earthquake is indicated.

The island arc is situated around 200 and 400 km to the west of the trench, parallel to it. Its history is rather complex and two main volcanic fronts can be seen (Bouysse [16]). An early Eocene volcanism constitutes the older arc whereas the recent and still active arc settled several millions years after the older arc ceased its activity. South of Martinique, the recent volcanism re-occupied the same position than the older arc. However, from Martinique northwards, the recent arc is offset progressively from the older one to the west (Fig. 2.2). As a result of this, the eastern (Grande Terre) and western (Basse Terre) parts of the island of Guadeloupe are of different volcanic origin. This separation of the recent and older arcs is proposed to be the result of kinematic changes in the subduction processes (Bouysse and Westercamp [17]). The trench of the subduction is filled mainly with sediments coming from South American rivers as the Amazon and Orinoco. The consequence of this huge sedimentary input is the presence of an important sedimentary prism. The accretionary prism width increases to the south and shows a maximum thickness of 20 km (Westbrook, [139], [140]) at the Barbados accretionary prism. It is a strong negative magnetic anomaly (Bowin [18]), observed at 150 km to the east of the present volcanic front, that indicated the location of the contact between the Caribbean and the subducted Atlantic crust. This subduction zone is characterized by a slow convergence rate and the subduction of a relatively old oceanic crust (Lower Campanian-Maestrichtian). Another characteristic of the subducting plate is the presence of several

fracture zones initiated at the Mid-Atlantic ocean ridge. Three WNW-trending ridges of the Atlantic oceanic crust are presently being subducted beneath the Lesser Antilles. The 450 km long and 30-50 km wide Barracuda and the 150 km long and 30-40 km wide Tiburon ridges have a bathymetric expression seaward of the Barbados accretionary complex. They are gravimetrically uncompensated and interpreted as fracture zones related to the segmentation of the mid-Atlantic spreading centre. To the South, the St Lucia ridge is buried beneath a blanket of sediments but has been recognized by seismic reflection. The interaction of these Atlantic bathymetric features with the leading plate margin has induced a series of effects on the evolution of the island arc. The frontal collision of the ridges with the facing arc crust may produce a horizontal compression, a change in the topography of the contact between the two lithospheres (interplate contact) and possibly a change in coupling between the plates.

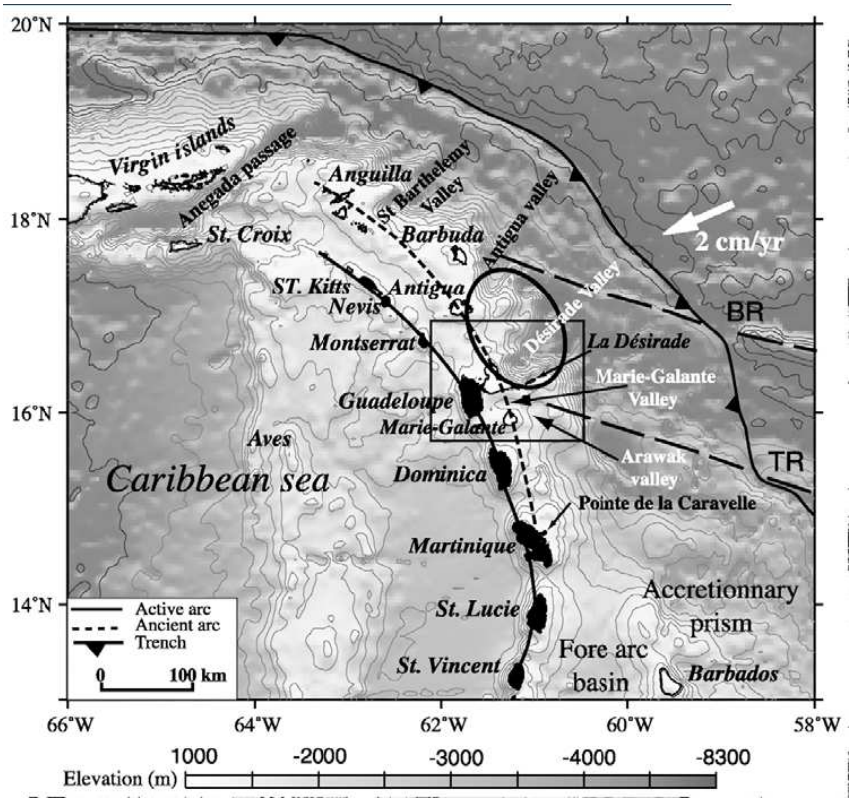

Fig. 2.2: Bathymetric map of the Lesser Antilles arc [44]. Bathymetry from Smith and Sandwell [112], contour interval, 500 m. Continuous black line, recent volcanic arc; dotted black line, ancient arc. Volcanic islands (on recent arc) in black; coral reef islands (on ancient arc) in white. Black dashed lines mark Barracuda (BR) and Tiburon ridges (TR).

Another particularity of this region is the presence here of the limit between the North American plate (NAM) and the South American plate (SAM). First, the Barracuda ridge was thought to be the boundary limit (Bowin [18]). Later, Bouysse and Westercamp [17] propose a diffuse boundary as large as the Lesser Antilles arc. Recently, GPS measurements (DeMets et al.[33]) and mapping of active faults (Feuillet et al.[44]) at sea show a deformation North of 16°N, with a trench parallel component of sinistral shear that decreases south-eastward from 15 to 4 mm/yr seaward of Guadeloupe. South of Guadeloupe, if the SAM/CAR plate motion vector (Weber et al.[136]) is used, no slip partitioning exists in the southern part of the arc, consistent with the vanishing of the observed sinistral slip partitioning (Feuillet et al.[44]). The central part of the eastern Caribbean subduction is known for its volcanic activity. In 1902, an eruption of the Montagne Pelée in Martinique killed 30,000 people. Since 1996, the Montserrat volcanoe is active and devastated a part of the island.

2.1 Seismic hazard in the Antilles Arc

The seismicity level of the Lesser Antilles is rather low for an active margin, and it is at least partly due to the slow convergence rate (ca. 2 cm/yr). Nevertheless the Caribbean arc experienced several large (M>7) historical earthquakes : 5 April 1690, Nevis, 8 February 1843, Guadeloupe, 18 November 1867, Virgin Islands, 8 October 1974, Antigua (Fig. 2.3); some of them apparently rupturing the plate interface.

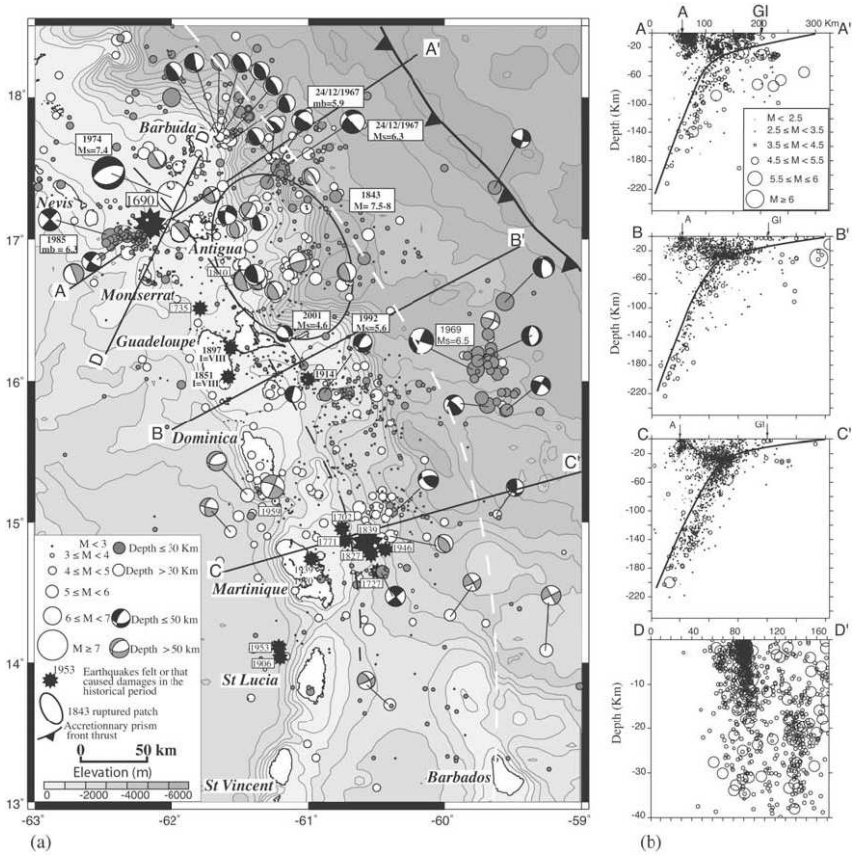

Fig. 2.3: (a) 1950-2001 seismicity in Lesser Antilles arc. (b) Distribution of regional seismicity recorded by Guadeloupe and Martinique regional networks (IPG), after (Feuillet et al.[44]).

Until recently the Benioff zone of the Lesser Antilles arc was poorly defined. The hypocenter depths increase westward, from a few kilometers near the trench down to 200 km in the subducted slab beneath the western arc (Dorel [36]). The plate interface dips at a low angle west of the trench and much more steeply under the arc with a marked flexure offshore the outer islands (Fig. 2.3). The seismicity level is higher in the northern part of the arc where some historical earthquakes of large magnitude (M>7.5) have been recorded (Robson [104]; Sykes and Ewing [127]; Dorel [36]; Stein et al. [124]; Feuillard [43]; Bernard and Lambert [13]; Dziewonski et al.[38]). This has probably to be correlated to the interaction of the Barracuda and Tiburon ridges (asperity effect) with the subduction zone. Whether these ridges, and especially the Barracuda Ridge, generate mainly interplate thrust fault earthquakes or only intraplate normal faulting events still remains a matter of debate. Based on general considerations seismic coupling is supposed to be weak, in spite of the occurrence in 1843 of a large earthquake, north of Guadeloupe Island, that destroyed Pointe-a-Pitre city. This event was probably a mega-thrust earthquake (M>7.5) located at the interplate. The subduction segment of North Sumatra has also been considered by experts as largely aseismic up to 1993 but nevertheless the M=9 mega-thrust earthquake of 26/01/2004 occurred in this area.

2.2 Previous experiments

Many studies were conducted in the southern part of the Lesser Antilles arc but only few were conducted in the central and northern part of the arc. In 1999, during the Aguadomar cruise on-board R/V Atalante, swath-mapping bathymetry, single channel seismic reflection and gravity was acquired on the Lesser Antilles island arc from Antigua to Martinique (Fig. 2.4, e.g. Le Friant et al.[82]). The Institute for Geophysics of the University of Texas at Austin conducted a first seismic experiment, involving multichannel seismic acquisition and OBS deployments in 1998 (Bangs et al. [8], Christeson et al. [26]).

- SISMANTILLES I: Elements of the Seismic Structure and Activity of the Lesser Antilles Subduction Zone (Guadeloupe and Martinique Islands) from the SISMANTILLES Seismic Survey

The SISMANTILLES I project was carried out at a regional scale for a first reconnaissance of the seismic structure and activity from northern Guadeloupe to Martinique islands. The project focused more particularly on the

detection, mapping and characterization of the potentially seismogenic part of the interplate subduction fault. The french N/O Nadir vessel acquired 2500 km of deep-penetration multichannel reflection seismic (MCS) profiles (Dec 01- Jan 02). Up to 37 3-component Ocean Bottom Seismometers (OBS) from ISV-Hokkaido and Géosciences Azur were deployed offshore over several weeks together with a set of 3-component broad-band stations on the islands (Martinique, Dominica, Guadeloupe and Antigua). These instruments recorded continuously both the MCS shots that provided wide angle reflection and refraction (WARR) data as well as the local, regional and teleseismic earthquakes. On MCS profiles, reflections from the top of the subducting oceanic crust and decollement can be followed down to several kilometers depth beneath the thick accretionary prism. Detailed velocity analysis provided depth structural sections that are used as an input for the forward modeling of WARR data. Thanks to these data, we can constrain on 3 transects to the arc, the part where the forearc deep crust is in contact with the subducting oceanic plate, considered as a proxy for the seismogenic part. Its location with respect to the deformation front and the volcanic arc and its downdip size appear significantly variable along the arc. The local earthquakes now reliably located in map and depth thanks to the high-quality P and S observations of the OBS network can be discussed with respect to these imaged structures. Local earthquake P & S tomography as well as receiver functions analysis which are in progress will bring more constraints on the deeper structure beneath the arc crust and thus on the downdip limit of the seismogenic portion of the subduction interplate. The Antilles have the worldwide thickest accretionary wedge blanketing the objective, which is the interplate boundary beneath, and has the most heterogeneous and complex lower plate. This may have been a handicap.

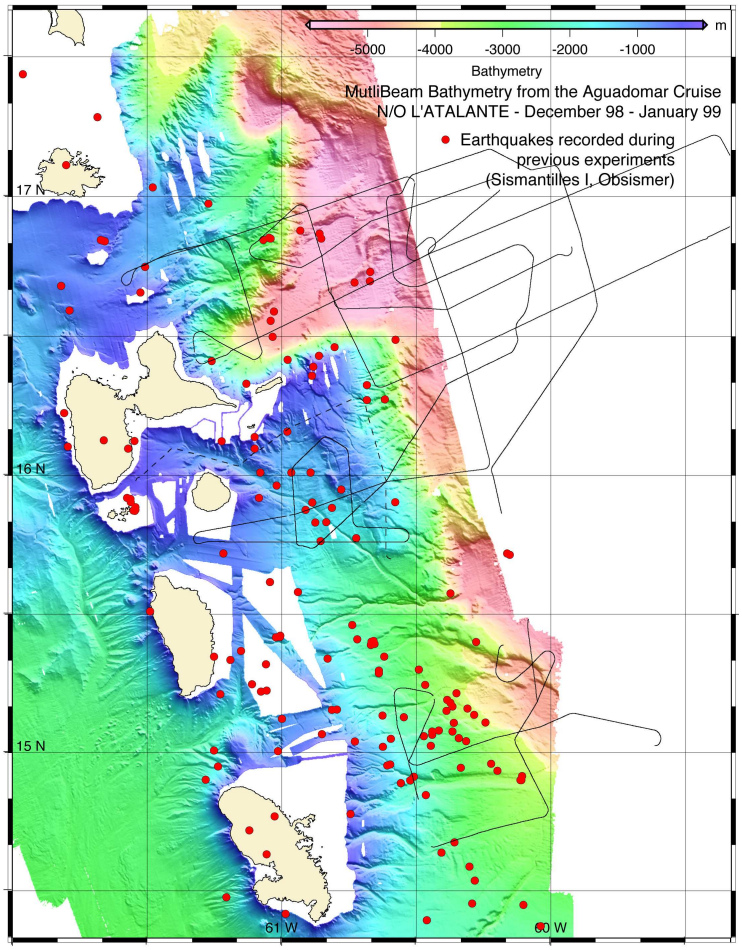

Fig. 2.4: Bathymetric map acquired during the Aguadomar experiment 2003. Earthquakes located during previous experiments (Sismantilles, Obsismer) are shown by red dots. Location of MCS lines shot during the Sismantilles I experiment are shown in black.

However the feasibility study SISMANTILLES I has shown examples of acceptable penetration and imaging with MCS reflection and OBS refraction, though not for all the lines of course. Also, an efficient recovery of high-quality earthquake signals obtained by OBS has been demonstrated, but seismic activity is moderate. Earthquake

data that will be recorded also during SISMANTILLES II that is targeted on artificial source recording, will be a complement to this previous one.

- OBSISMER: project of continuous observation of the earthquakes at sea

In the framework of a contract between the French government and Martinique, the IPG Paris and Géosciences Azur conducted the deployment of OBSs for continuous observation of the earthquakes at sea offshore Martinique. It aims at following the variability of the seismicity over a long period but then necessarily in a limited area. A network of 8 OBS (Ocean Bottom Seismometers) was deployed since November 2005 in the North-East of Martinique for periods of 4 months.

2.3 Aims of the project

Subduction earthquakes constitute the greatest seismic and tsunami hazard in the Antilles. A quantitative approach of hazard assessment requires a seismological, geophysical and geological observation experiment. In order to fulfill a gap of observations in this field several experiments were programmed at sea during 2007 to improve the estimation of the potentially interplate seismogenic zone, the existence and the time of return of the very large past earthquakes and on the state of constrain of the seismogenic zone. The main goals of the Sismantilles 2007 project are to map the location, size and spatial variation of the potential seismogenic zone, by a grid of reflection-refraction profiles, whose location and parameters are defined with the help of the first reconnaissance (Sismantilles I) experiment. MCS reflection seismics can resolve the updip limit of the contact between the forearc crust and the downgoing plate, that is a proxy to the updip limit of the seismogenic zone. Here a sampling of the variability along the arc by 14 dip-lines of 90 km length is planned. OBS refraction can penetrate to the forearc mantle and thus provide Pn waves with which to define the downdip limit of the contact between its crust and the incoming plate, which is a proxy to the downdip limit of the seismogenic zone. 4-5 strike-lines 180 km long, with OBS at crosspoints with the dip-lines are planned. Surveying along the arc will add to the estimate of the location and downdip size of the seismogenic zone and its spatial variability, that is its segmentation and hence complement the assessment of potential size of quakes. The distribution of seismic activity with respect to these structures will allow to improve the model. The present experiment MSM-04/2-OBSANTILLES consists in the shooting of two dense refraction profile across the island arc and the accretionary prism and the deployment of dense networks of marine seismometers (OBS). During the Sismantilles II experiment, on-board the R/V Atalante, deployment of some extra OBSs in the north of the area, shooting with a large seismic source and finally MCS data acquisition was conducted in February 2007. The OBS network will then be recovered from the R/V Antea (IRD) in April 2007 and in June from a rented vessel. The project is supported by the French Agence National de la Recherche¡ in the framework of the call ´Catastrophe Tellurique et tsunamis´ (project Subsismanti) and by the European STREP ´Thales Was Right´ (FP6-2004-NEST-C-1 INSIGHT : Transients in the Hellenic and Antilles Loci of Earthquakes of European Subductions: Water Activity, Structure and Seismic Risk Illuminated by Geophysical High-Technology).

3 Participants

3.1 Scientists - MSM 04 Leg 2

1.	Prof. Dr. Ernst Flüh	IFM-GEOMAR
2.	Alain Anglade	GéoAzur
3.	Dr. Anne Bécel	IPG
4.	Dr. Warner Brückmann	IFM-GEOMAR
5.	Wiebke Brunn	IFM-GEOMAR
6.	Dr. Philippe Charvis	GéoAzur
7.	Anke Dannowski	IFM-GEOMAR
8.	Olivier Desprez	GéoAzur
9.	Yvonne Dzierma	SFB-574
10.	Dr. Audrey Galve	GéoAzur
11.	Julia Mahlke	SFB-574
12.	Yann Hello	GéoAzur
13.	Dr. Audrey Gailler	GéoAzur
14.	Helge Johnson	UBDES
15.	Aleksandre Kandilarov	UBDES
16.	Eric Labahn	KUM
17.	Alexander Labrenz	IFM-GEOMAR
18.	Marten Lefeldt	SFB-574
19.	Dr. Cord Papenberg	IFM-GEOMAR
20.	Wendy Pérez Fernández	IFM-GEOMAR
21.	Martin Pieper	SFB-574
22.	Dr. Lars Planert	IFM-GEOMAR

3.2 Crew MSM 04 Leg 2

1.	Karl Friedhelm von Staa	Master
2.	Holger Leuchters Chief	Mate
3.	Theo Griese	1st Officer
4.	Thomas Knak	2nd Officer
5.	Thomas Ogrodnik	Chief Engineer
6.	Manfred Boy	2nd Engineer
7.	Kurre Klaus Krüger	Motorman
8.	Martin Tomiak	System Operator
9.	Gerd Neitzel	Electrician
10.	Frank Riedel	Electronics
11.	Helmut Friesenborg	Fitter
12.	Norbert Sieber	Chief Cook
13.	Waldemar Arndt	2nd Cook
14.	Norbert Kreft	Bosum
15.	Hardy Schwieger	A/B
16.	Gerhard Müller	A/B
17.	Alexander Rathgeber	A/B
18.	Rainer Badtke	A/B
19.	Dieter Jürss	A/B
20.	Thomas Scheibe	A/B

Fig. 3.1: Participants of the Merian Cruise MSM 04/2

4 Agenda

The cruise MSM04/2 started on January 03, 2007 in Fort-de-France, Martinique. All together 22 scientists embarked on Maria S Merian, comprising the international group of scientists from Bulgaria, Costa Rica, France, Germany and Norway. The ship left port at 10:30 03.01, and after a short transit of only 3 hours the deployment of 50 Ocean Bottom Seismometers and Hydrophones (OBS/OBH) began. Instruments were deployed at a spacing of 2.5 nm on average; all 50 instruments were deployed within 24 hours. Subsequently, across the 150 nm long spread of instruments an airgun array consisting of three 16 liter and two 32 liter guns were fired with a triggerintervall of 60 s at a ship's speed of 4.0 kn on average, resulting to a shot spacing of 100 m. For the second half of the profile the streamer was also deployed. Shooting terminated at 06:00 on 06.01., and subsequently instruments were recovered. The Cruisetrack can be seen in Fig.4.1. Four instruments remained at the seafloor for earthquake monitoring. Instrument recovery lasted until the morning of 08.01., and was interrupted for a few first trials to test the pore pressure device.

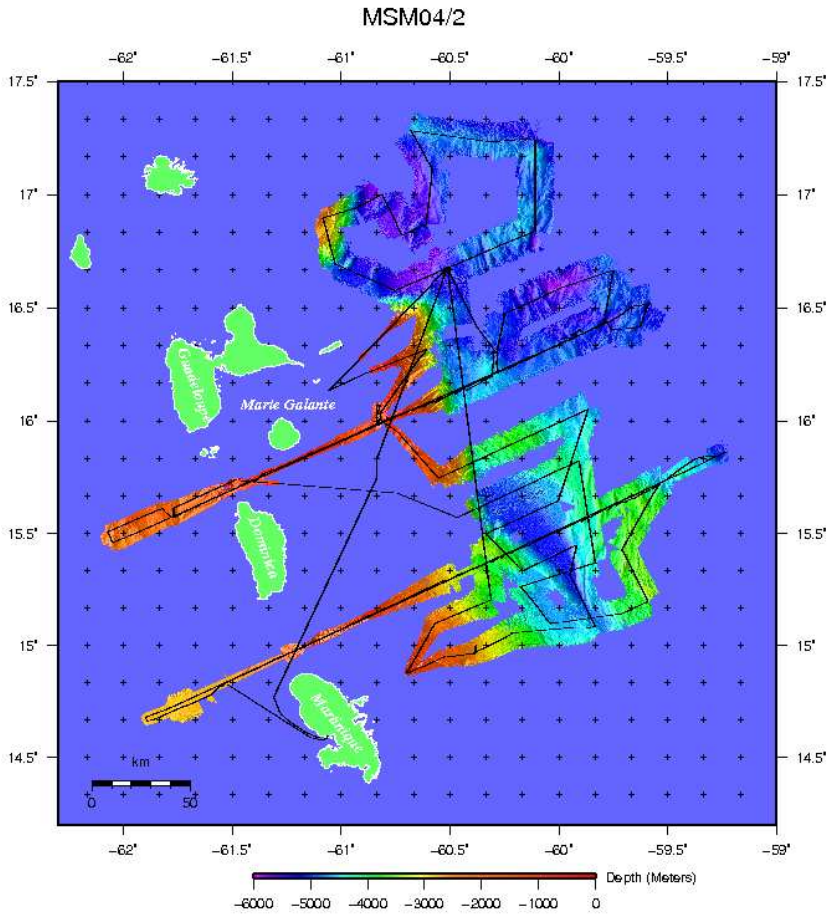

Fig. 4.1: Cruisetrack MSM 04/2

After profile 01 was completed, altogether ten OBS were deployed for earthquake monitoring, and two were recovered for maintenance from the existing network. On Tuesday, 09.01., the pore pressure device was finally tested successfully at water depth of nearly 2000m. Thereafter, 44 instruments (OBH61 to OBS104) were deployed along the second profile north of the Republic of Dominica. Shooting was started at 13:30 10.01. with four airguns in operation, a fifth airgun was deployed five hours later. The streamer was deployed for the western part of the profile only. The profile was shot at a speed of 3.7 kn on average, again with a 60 s trigger interval. At 06:00 on 12.01. this was terminated, and instrument recovery started imedeately afterwards. Six instruments, that

also formed part of the long term seismological network were not recovered. Recovery was finished midday on 14.01., but was interrupted by several GCPP samples at different water depths, including a location on a mud volcanoe in 5000 m water depth. We then started to deploy the instruments for the seismological network north of profile 02. During this deployment another GCPP measurement was made on the mud-volcanoe sampled before. Further on, we realized that a broad band seismometer had been deployed with a recorder that only allows high frequency energy to be digitized. It was decided to pick up and redeploy this instrument (OBS111). However, upon the interrogation with the release command the instrument responded well, but did not rise from the seafloor and remained at 5200 m depth. After several tries this instrument was abandoned. In the morning of 16.01 all instruments in the northern part had been deployed. Attempts to find a suitable location for the pore pressure long time monitoring lander failed.

In the evening of 16.01 the first of the remaining 8 instrumnets south of Profile 02 was deployed. On 17.01 the remaining OBS were deployed , and recovery of six French instruments deployed before the Merian Cruise was attempted. Unfortunately, one instrument did not respond and was also abandoned.. The pore pressure lander was also deployed for a five to six month long observation period.

On 18.01 another attempt was made to recover OBS111, but again although the instrument did respond, it did not rise to the surface. In the morning of 19.01 at 08:00 the pilot entered the Merian, and soon after Merian birthed in Martinique, terminating cruise MSM04-2.

5 Scientific Equipment

5.1 OBH/OBS Seismic Instrumentation

The Ocean Bottom Hydrophone (OBH)

The first IFM-GEOMAR Ocean Bottom Hydrophone was built in 1991 and tested at sea in January 1992. This type of instrument has proved to have a high reliability; more than 4000 successful deployments were conducted since 1991. A total of 5 OBH and 25 OBS instruments were available for MSM04-2. Altogether 60 sites were deployed for refraction seismic profiles and additionally 20 stations for the long-term seismological network during the MSM04-2 cruise. The principle design and a photograph showing the instrument upon deployment are shown in Fig. 5.1. The design is described in detail by Flüh and Bialas [48].

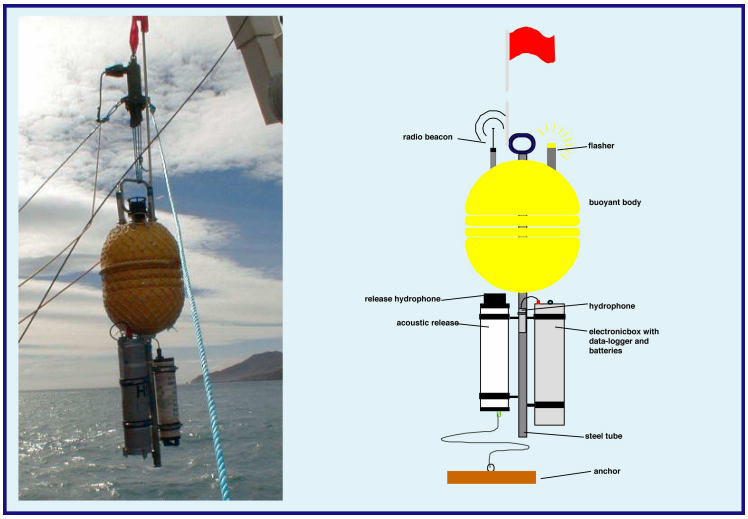

Fig. 5.1: Principle design of the IFM-GEOMAR OBH (right panel, after Flüh and Bialas [48]) and the instrument upon deployment (left panel).

The system components are mounted on a steel tube, which holds the buoyancy body on its top. The buoyancy body is made of syntactic foam and is rated, as are all other components of the system, for a water depth of 6000 m. Attached to the buoyant body are a radio beacon, a flash light, a flag and a swimming line for retrieving from aboard the vessel. The release transponder for the acoustic release is also mounted here. The sensor is an E-2PD hydrophone from OAS Inc., or a HTI-01-PCA hydrophone from HIGH TECH, and the recording device is an MBS, MES, MLS or MTS recorder of SEND GmbH, which is contained in its own pressure tube and mounted below the buoyant body opposite the release transponder (see Fig. 5.1). The different recorder systems are developed to serve a variety of seismic recording and power consumption requirements. Therefore, the available recording sampling rate reaches from 0.1 Hz for seismological observations to the 50 Hz range for refraction seismic experiments and up to 10 kHz for high resolution seismic surveys. For the purpose of low-frequency recordings such as seismological observations of earthquakes during long-term deployments the deployment period can be extended to about one year.

The IFM-GEOMAR Ocean Bottom Seismometer 2002

The IFM-GEOMAR Ocean Bottom Seismometer 2002 (OBS-2002) is a new design based on experiences gained with the IFM-GEOMAR Ocean Bottom Hydrophone (OBH; Flüh and Bialas [48]) and the IFM-GEOMAR Ocean Bottom Seismometer (OBS, Bialas and Flüh [49]; see Fig.5.2). The basic system is constructed to carry a hy-

drophone and a small seismometer for higher frequency active seismic profiling. However, due to the modular design of the front end it can be adapted to different seismometers and hydrophones or pressure sensors. For the seismological network 3 stations were equipped with gimbaled Spahr Webb seismometers and one station with a gimbaled PMD sensor. For these stations, the hydrophone was replaced by a differential pressure gauge (DPG) as described by Cox et al [27]. The sensitive seismometer is deployed between the anchor and the OBS frame, which allows good coupling with the sea floor. The three component seismometer (KUM), usually used for active seismic profiling, is housed in a titanium tube, modified from a package built by Tim Owen (Cambridge) earlier. Geophones of 4.5 and 15 Hz natural frequency were used during MSM04-2. While deployed to the sea floor the entire system rests horizontally on the anchor frame. After releasing its anchor weight the instrument turns 90° into the vertical and ascends to the surface with the floatation on top. This ensures a maximally reduced system height and water current sensibility at the ground (during measurement). On the other hand the sensors are well protected against damage during recovery and the transponder is kept under water, allowing permanent ranging, while the instrument floats to the surface.

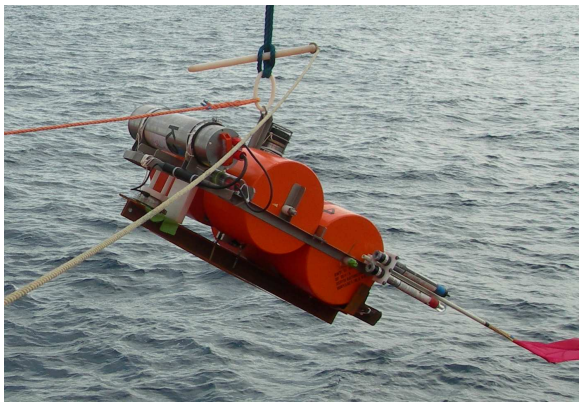

Fig. 5.2: IFM-Geomar OBS (2002 Design)

The ≪Hippocampe≫ OBS of Géosciences Azur

The study of continental margins, subduction zones and oceanic basins as well as the quantitative assessment of seismic hazard near densely populated coastal areas request the deployment of a large number of Ocean Bottom Seismometers (OBS) during a period of several weeks for active tomography, and up to several months for passive experiments. Geosciences Azur (joint IRD1, CNRS2, UPMC3 and UNSA4 laboratory) developed a new, easy-to-use, 4-components OBS named Hippocampe (Fig.5.3). The Hippocampe OBS exists in a short period version based on 3 gimbaled, 4.5 Hz, geophones installed in their own, 150 mm diameter, glass sphere. The broadband sensor was designed in cooperation with Guralp System, on the basis of a CMG-40T seismometer gimbaled in a similar glass sphere, with a magnetometer and tiltmeter for position on the bottom (option). The data logger developed at Geosciences Azur consists in a 24 bits analog/digital converter synchronized by a high accuracy Seascan clock (2 10-8). Data are buffered in a 128 Mb to 1 Gb flash memory then stored on a 40 Gb hard disk. Power consumption is 500 mW for continuous recording of 4 channels at 200 samples per seconds allowing 6 to 12 months recording autonomy on the sea bottom. The data logger and batteries fit in a 432-mm diameter glass sphere. A second sphere is used to increase the floatability during long-term deployment.

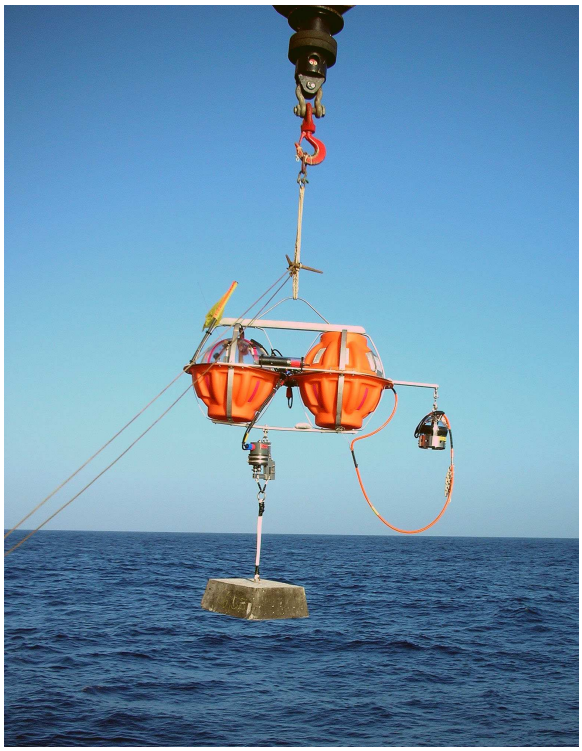

Fig. 5.3: Hippocampe OBS

For recovery an acoustic code trigger simultaneously an electro-mechanical release system, developed in cooperation with Guralp System) and an electrolytic, burn-wire, release. At the surface flash lights and radio beacons allow an easy recovery of the instrument at sea. These new instruments were used for the first time during the Esmeraldas experiment (2005) to study the 3-D structure and seismic activity of Ecuador subduction zone, a network of 20 Hippocampe OBSs was deployed, together with 7 OBSs from the previous generation and 30 land-seismometers during more than 3 months. This network recorded successfully shot of the 128-liter airgun source towed by R/V Atalante and numerous earthquakes. For this first deployment the new Hippocampe OBS provide excellent results, with 100% recovery, and an excellent coupling with the sea bottom especially for horizontal

components. Since that time several active (e.g. Encens in the Gulf of Aden, 2006) and passive (Rosmarin in the Ligurian sea and OBSISMER offshore Martinique) experiments were conducted at sea. 10 extra Hippocampe OBS were built for permanent monitoring of seismicity offshore Martinique and successfully deployed since November 2005. The OBS operated by Geosciences Azur is part of the French OBS pool supported by IFREMER, CNRS and IRD which allow to share the 80 instruments available in the French community.

Tab. 5.1: ≪Hippocampe ≫ OBS Characteristics

External Sensor	3 geophones 4,5Hz gambled 3 components 30 s type CMG-40T Hydrophone Hightech 1 Hz
Band Pass	4,5 - 100 Hz 0,033 Hz - 100 Hz
A/D converter	24 bits high dynamic range with wide range sampling rates
Sampling rate	1 to 255 ms by step of 1 ms
Number of channels	1 to 4
Clock accuracy	1 Seascan SISMTB clock - 2 10-8 GPS synchronization before and after immersion
OBS position	10 m, Water wave computing. Acoustic positioning (12 kHz) possible
OBS orientation	1° using water wave propagation triaxial magnetometer and tiltmeter need to be validate (Guralp CMG-40T)
Processor	1 CPU persistor CF1, CF2
Buffer memory	128 Mo to 1 Go flash memory card
Acquisition Mode	Continue
Acquisition Storage	40 Go IDE (interface USB2.0 for data back-up from outside the sphere) 4 Go flash memory card
Electrical consumption Autonomy	∼500 mW 4 channels at 200 samples per second 6-10 month in continuous acquisition mode
Batteries	Function of acquisition length: for 3 months: 16 DD cells (NB: twice D size capacity), 6 C cell lithium 4 cell C size - 2 * 9V and 24 AA alkaline
Container	**Main container** 17 glass sphere diameter (432 mm). A second 17´ glass sphere can be added to increase buoyancy and to encapsulate extra batteries for long-term deployment. **Sensor container** 6´ glass sphere diameter (150 mm)
Weight	100 kg before deployment: 45 kg at recovery
Maximum depth	7 km
Recovery	**Release command** Edgetech acoustic (2 encoded channels with transducer and ranging mode) Benthos acoustic (Receive only hydrophone) Main and Back up programmed clock. **Release function** Electrical release mechanism (Guralp) Mechanical electrolytic (Burn wire) Release **Recovery Aids** VHF radio Beacons Strobe lights

5.2 GCPP (Gravity Corer Pore Pressure)

Introduction

During MSM04-2 a newly developed tool for measuring in situ pore pressure was tested for the first time. The so called Gravity Corer Pore Pressure tool (GCPP) was developed within the framework of the Cooperative

Research Center (SFB574) in Kiel (Fig.5.4). Intended for use in areas with high rates of fluid advection the GCPP combines a standard geological corer for sediment sampling with a highly sensitive device for measuring differential pore pressures. The technical concept of the pore pressure component is based on earlier designs such as the PUPPI (Pop Up Pore Pressure Instrument, Schultheiss [115]) which have employed a throw-away bottom assembly combined with recoverable data packages. In the GCPP a Keller differential pore pressure sensor with a battery package and a data logger is integrated into the weight package of the gravity corer (Fig.5.5(b),5.5(d)).

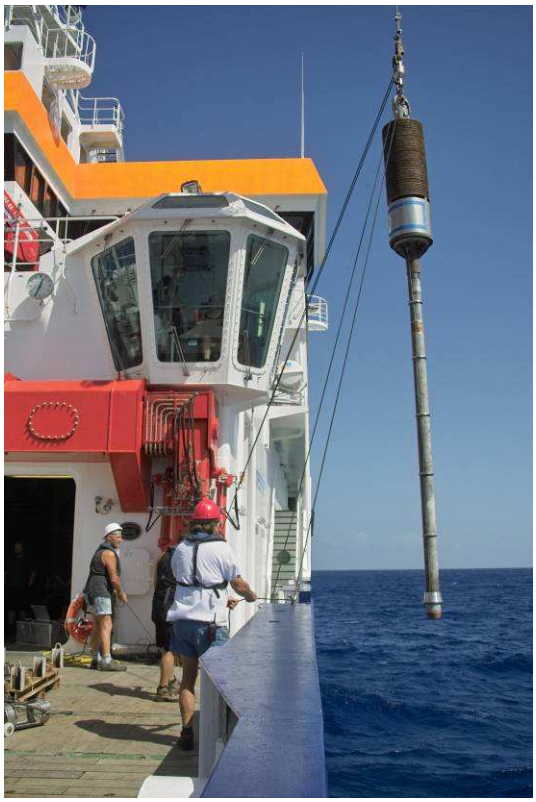

Fig. 5.4: GCPP deployment, the bottom of the corer weight houses the electronics package; rings visible around the corer provide guidance for the pipe connecting the pressure sensor to the tip of the corer;

The differential pore pressure sensor is connected to a specially formed head above the cutting shoe of the corer, which displaces a defined volume of sediment, generating a spike in pore pressure. The dissipation pattern and decay rate of this pressure peak can be used to approximate permeability and residual pore pressure over the sediment interval near the tip of the tool.

GCPP Deployments during MSM04-2

The advantage of using the GCPP tool is that the depth interval over which pore pressure is measured is also cored and recovered, so that the sediments from this interval can be subjected to geotechnical and hydrological testing. Therefore, during MSM04-4 most cores recovered from successful test were not split to retain sufficient amounts of undisturbed material for hydrological and geotechnical testing in shore based laboratories.

5.3 PWPL (Porewater Pressure Lance) Lander

Introduction

To better understand the fluid dynamics of mud volcanoes and other fluid release features the PWPL (Porewater Pressure Lance) Lander was designed and built within the framework of the Cooperative Research Center (SFB) 574 in Kiel. The PWPL is able to monitor variations in fluid expulsion and possible correlation with local seismicity. It detects pore pressure changes along a profile in the shallow subsurface using a 2m long stinger with 4 pressure ports (Fig.5.5(a), 5.5(c)). Using a standard IFM-GEOMAR lander the tool can be precisely positioned on and slowly pushed into the seafloor. It can remain on the seafloor for several weeks or months in autonomous mode before being retrieved. Previous deployments from a few days to 2.5 months were carried off Central America and in the Gulf of Cadiz.

Deployment and tool configuration

Normally the PWPL is deployed by a standard video-guided GEOMAR deep sea lander, by which it can be positioned on very small fluid expulsion features (e.g. bacterial mats of m-scale). During MSM04-2 the PWPL was deployed using a wire release (free fall) system, The PWPL was lowered by wire to about 25m above the sea floor at the intended position when the releaser was activated and the system released.

The PWPL measures with two parallel sensors differential pressure between a reference port about 10cm above the sea floor and one of four ports on a 25mm diameter stinger at 50, 100, 150, and 200cm below the sediment-water interface (Fig. 5.5(b)). After deployment of the lander on the sea floor the stinger is slowly pushed into the sediment at a rate of 50 mm/minute. Pressure data are collected at 1 second intervals.

The PWPL was deployed on 16. January 2007 [UTC 21:28:16] at a water depth of 2685m about 75nm E of Martinique in an area with intense seismicity according to previous experiments (Sismantilles, Obsismer). The battery pack supplied is sufficient for 100 days of pore pressure measurements, logging will end on the 31. May 2007, the recovery of the PWPL is scheduled for early June 2007.

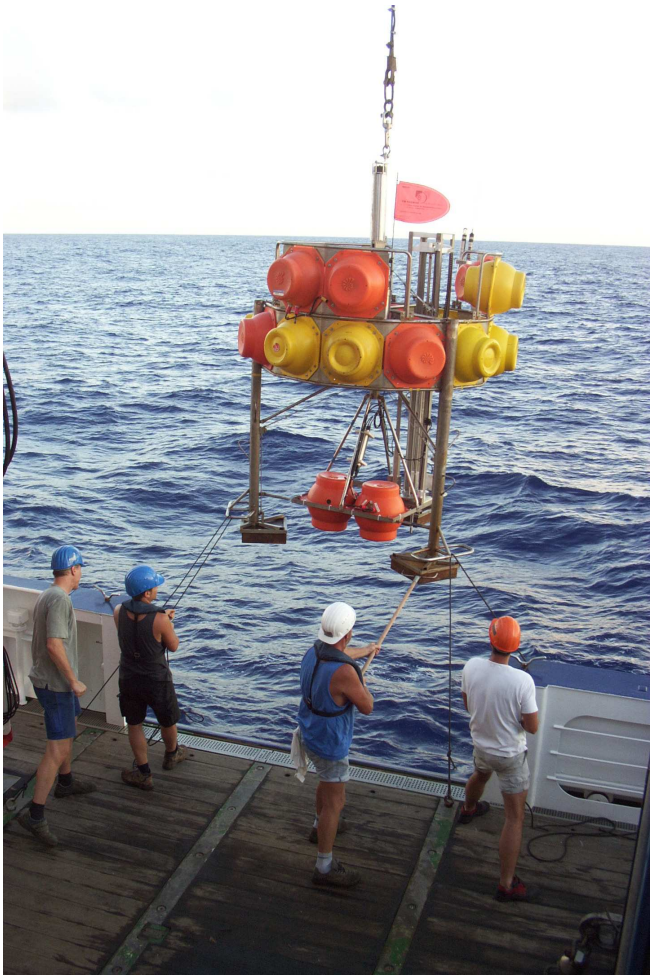

(a)

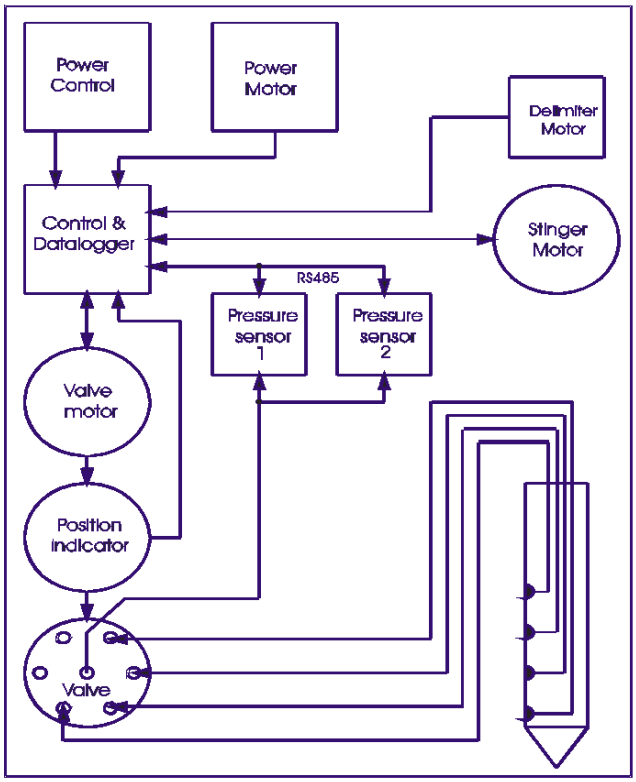

(b)

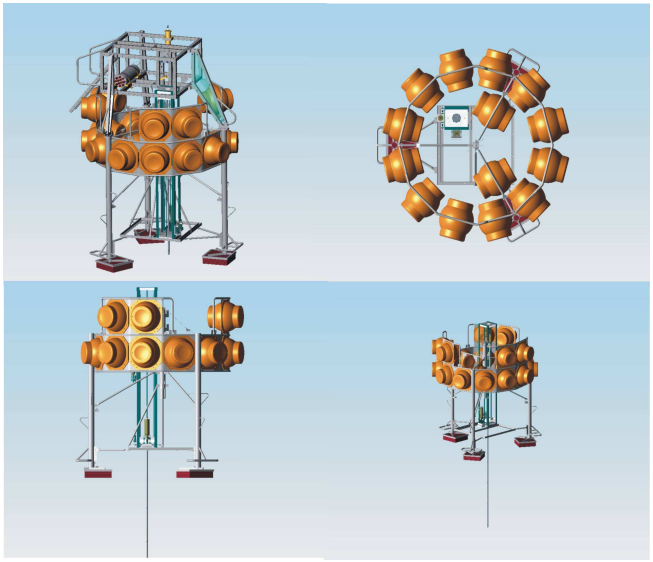

(c)

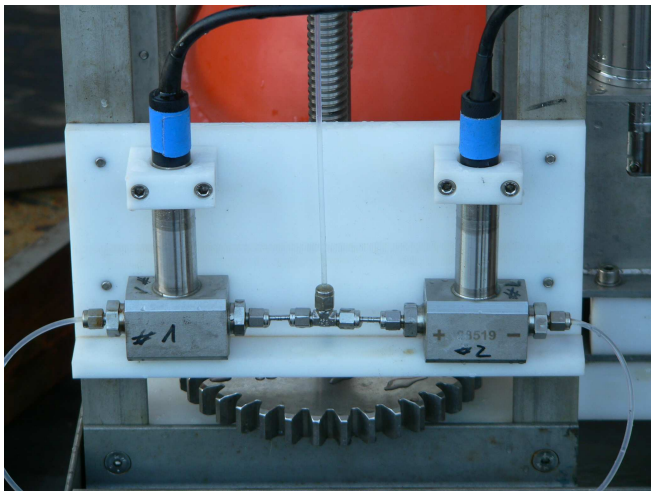

(d)

Fig. 5.5: (a) Deployment of PWPL Lander during MSM04/2;
(b) Schematic of internal tool control and data flow. Note that all pore pressure measurements are duplicated with two independent pressure sensors. The pressure ports are located at 50, 100, 150, 200cm below sea floor;
(c) Schematic of PWPL Lander in 3-D sketch; the lower two figures show the PWPL with extended measurement lance in perspective view;
(d) Differential pore pressure sensors, the center flow line is connected to the lance ports.

5.4 Airguns

GEOPHYSICAL EQUIPMENT:

- GUNCO gun controller (Figs.5.6 and 5.7(a))
- Ashtech GPS Mod. GG24
- 60 sec. shot-point interval
- 4.5 kn
- 5 single air-guns (Fig.5.7(b))
- 6 m air-gun depth for Bolt 800-CT
- 10 m air-gun depth for Bolt 1500 LL
- Distance from GPS antenna to centre of source: 47 m

ACQUISITION:
The survey was planned as two Profiles (Profile 01 and 02)

Profile 01:

From shot #1-101 the shot-point interval was 40 sec. For the rest of the line the shot-point interval was 60 sec. In the Field Data Log (FDL) it is remarked: Green (ok); normal fire. Yellow; the limit for out-of-range more then +/- 2 ms. Blue; manual tuning, gun set to fixed delay. Red; no sensor signal detected. From shot #329 gun #4 and #5 became yellow on the monitor. Decided to set both guns to manual tuning. Channel 5 on GUNCO (gun #5) did not accept the command.

Profile 02:

Before start of profile 02 the signal cable for gun #5 was replaced with a new one. At start/end of profile 02, a 20 min. test was performed, see remarks in (FDL). At start of line Gun #4 stopped shooting after one shot. Decided to bring the gun on deck. Due to a broken signal cable , gun #4 was replaced with the spare one from Bergen (1500 LL). From shot #371 all guns ok. There was no downtime due to bad weather conditions or errors in the seismic and navigation system.

Airgun Configuration:
Offset from GPS antenna to airguns = 47 m.

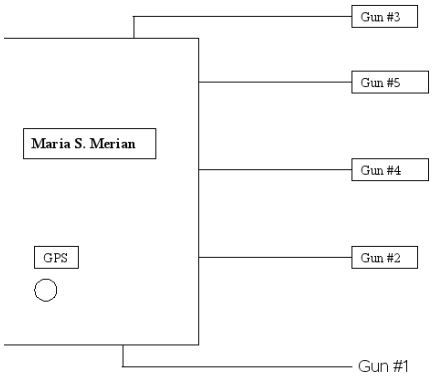

Fig. 5.6: Airgun Setup

Profile 01	**Profile 02**
Gun #1 = 20 liter	Gun #1 = 20 liter
Gun #2 = 20 liter	Gun #2 = 20 liter
Gun #3 = 20 liter	Gun #3 = 20 liter
Gun #4 = 32 liter	Gun #4 = 20 liter
Gun #5 = 32 liter	Gun #5 = 32 liter
Total = 124 liter	Total = 112 liter
Gun #1,2,3 = Bolt 1500 LL	Gun #1,2,3,4 = Bolt 1500 LL
Gun #4,5 = Bolt 800 CT	Gun #5 = Bolt 800 CT

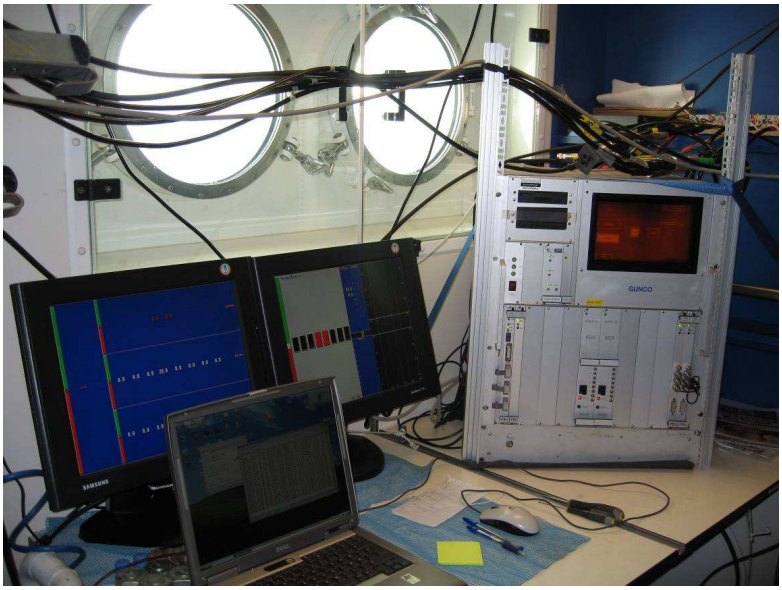

(a)

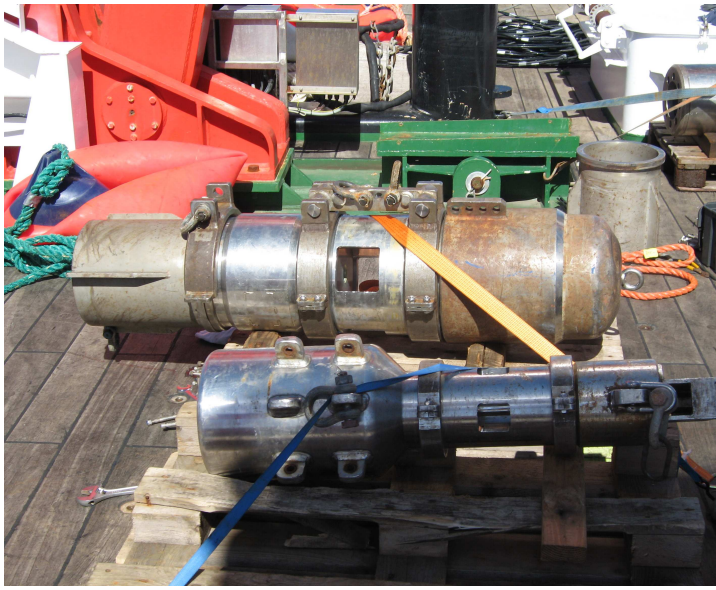

(b)

Fig. 5.7: (a)GUNCO gun controller (right). Lap Top for recording GPS (left).
(b)Bolt 1500 LL (in front) and Bolt 800 CT

6 Preliminary Results

6.1 Bathymetry

The EM120 system is a multibeam echosounder (with 191 beams) providing accurate bathymetric mapping up to depths exceeding 11000 m. This system is composed of two transducer arrays fixed on the hull of the ship, which send successive frequency coded acoustic signals (11.25 to 12.6 kHz). Data acquisition is based on successive emission-reception cycles of this signal. The emission beam is 150 ° wide across track, and 2 ° along track direction. The reception is obtained from 191 overlapping beams, with widths of 2 ° across track and 20 ° along it. The beam spacing can be defined as equidistant or equiangular, and the maximum seafloor coverage fixed or not. The echoes from the intersection area (2 °*2 °) between transmission and reception patterns produce a signal from which depth and reflectivity are extracted. For depth measurements, 191 isolated depth values are obtained perpendicular to the track for each signal. Using the 2-way-travel-time and the beam angle known for each beam, and taking into account the ray bending due to refraction in the water column by sound speed variations, depth is estimated for each beam. A combination of phase (for the central beams) and amplitude (lateral beams) is used to provide a measurement accuracy practically independent of the beam pointing angle. The raw depth data need then to be processed to obtain depth-contour maps. In the first step, the data are merged with navigation files to compute their geographic position, and the depth values are plotted on a regular grid to obtain a digital terrain model (DTM). In the last stage, the grid is interpolated, and finally smoothed to obtain a better graphic representation. Together with depth measurements, the acoustic signal is sampled each 3.2ms and processed to obtain a cartographic representation, commonly named mosaic, where grey levels are representative of backscatter amplitudes. This data thus provides information on the sea-floor nature and texture; it can be simply said that a smooth and soft seabed will backscatter little energy, whereas a rough and hard relief will return a stronger echo. On the cruise MSM04-2 Bathymetric data were collected in the region 17,5/14,5° N and -62,5/-59° W in proximity to Martinique and Dominica (the lesser Antilles). The EM120 was used continuously during cruise. Bathymetric data were processed partly on board during the survey and also after the cruise, using the academic software MB-System from Lamont-Doherty Earth Observatory. The data collected during MSM04 Leg 2 were merged with data collected during the cruises “Ewing”, “France”, SO154 and M35. Grids were computed with a grid-spacing of 30m. Corresponding maps are shown in Figs.6.1 and 6.2. The high resolution bathymetry collected on this cruise was also used to close gaps in the data of preceding cruises. Last but not least the data

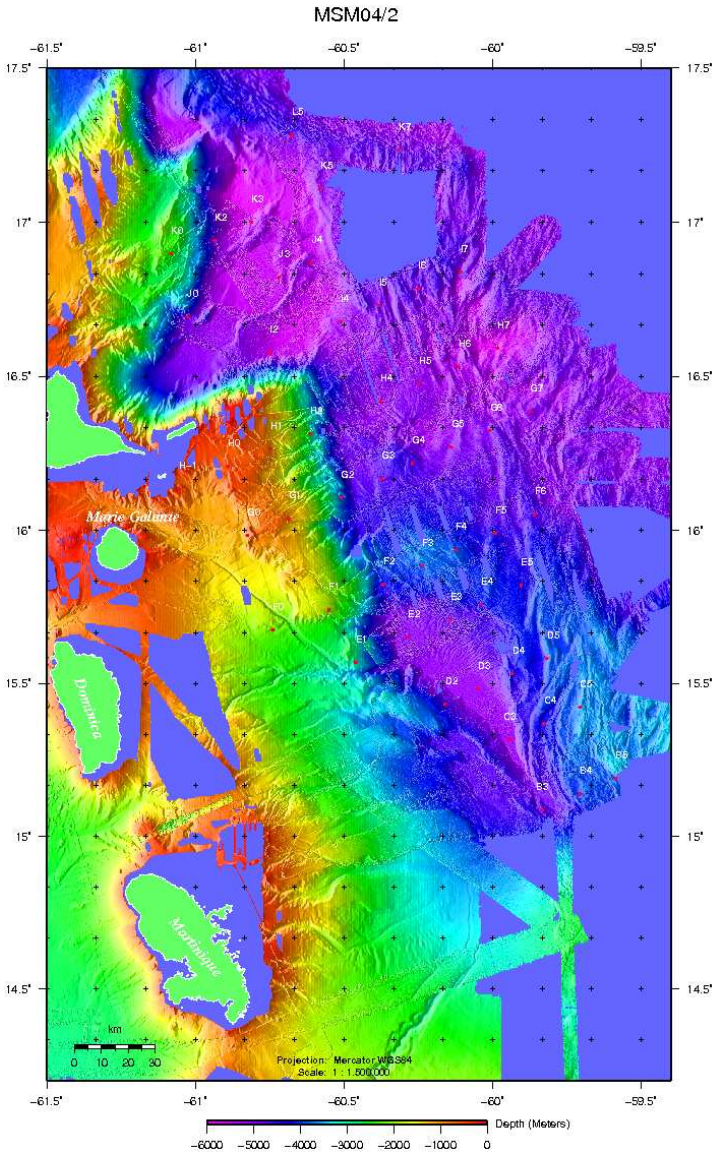

Fig. 6.1: Joint Bathymetry of Cruises Ewing and MSM04-2 and Seismological Network

were crucial to find locations to deploy the Lander and GCCPs.

6.2 Seismic Work

The main focus of the work during MSM04-2 was devoted to seismic work. Two wideangle seismic profiles across the island arc were acquired. In addition 50 OBS were deployed as a seismological network to be operational for four to six months, augmenting a dense array of landstations on the islands. In addition, 8 instruments that were already in operation had to be picked up and partially redeployed. In Fig. 6.1 a location map of the stations for the seismological network is shown. Fig. 6.2 shows the locations of the stations for the two wide-angle lines.

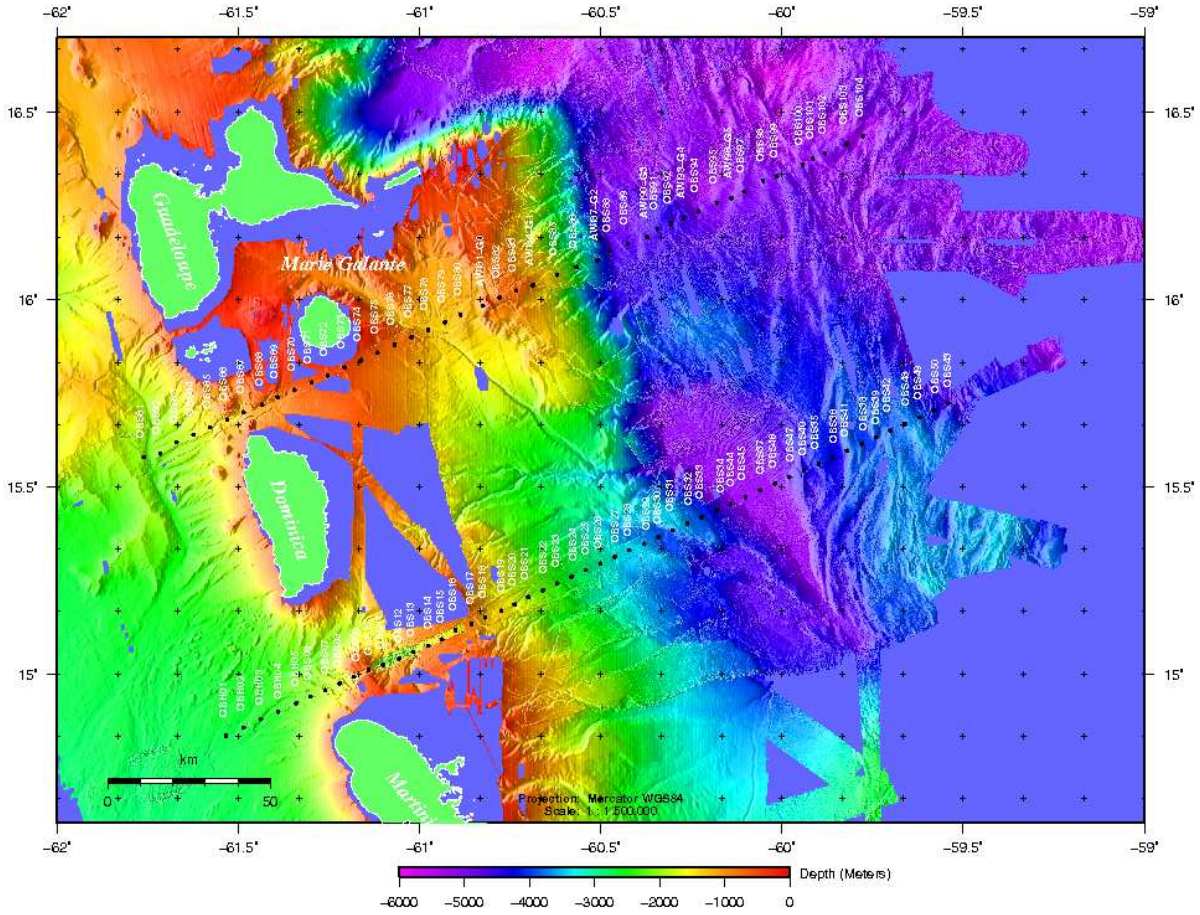

Fig. 6.2: Profiles 01 (S) and 02 (N)

6.2.1 Profile 01

A total of 50 Ocean Bottom Seismometers and Hydrophones (OBS/OBH) were deployed at a spacing of 2.5 nm on average on 03/04.01. Subsequently, extending for about 12 nm to both sides, across the 130 nm long spread of instruments an airgun array consisting of three 16 liter and two 32 liter guns were fired with a trigger interval of 60 s. With a ship's speed of 4.0 kn on average, the resulting shot spacing is just above 100 m. For the second half of the profile the streamer was also deployed. Shooting terminated at 06:00 on 06.01., and subsequently instruments were recovered. Four instruments remained on the seafloor for earthquake monitoring. Instrument recovery lasted until the morning of 08.01., and was interrupted for a deployment of the pore pressure device. The data are of excellent quality on average, with signal penetration up to 160 km. Only in the easternmost part, on the accretionary wedge, attenuation seems to be very high and seismic signals can rarely be seen in excess of 40 km. Two data examples are shown in Figs. 6.3 and 6.4 A four channel streamer was deployed for the western part of the line.

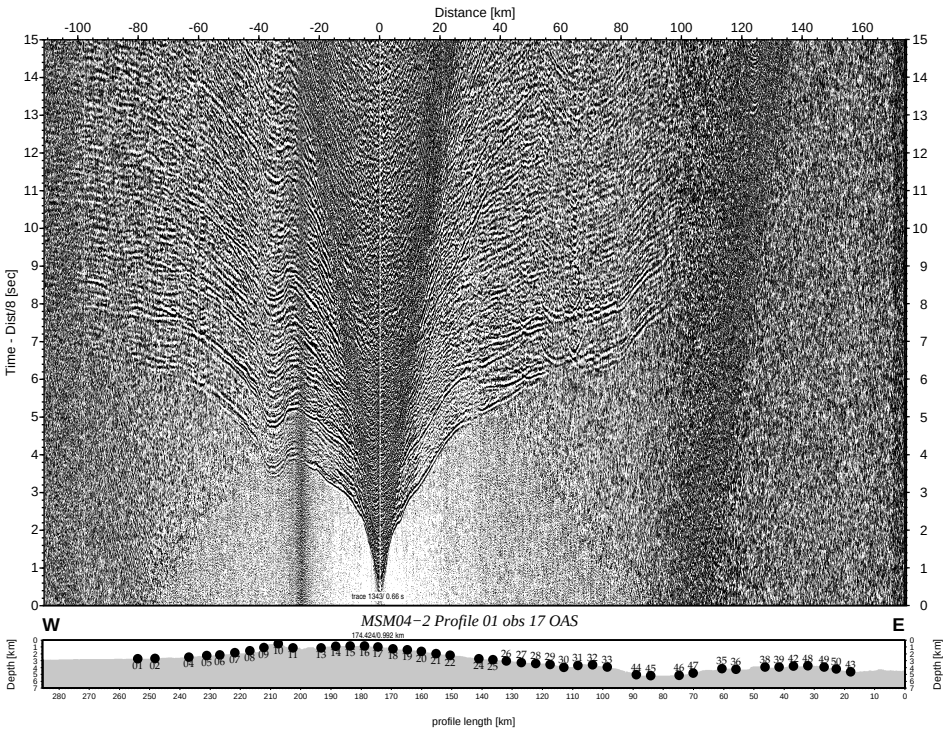

Figure 6.3.1.7l: Record section from obs 17 OAS, Profile 01.

Fig. 6.3: Record Section from OBS 17, Profile 01

6.2.2 Profile 02

For Profile 02 all together 44 instruments (OBH61 to OBS104) were deployed along the second profile north of the Republic of Dominica (see Fig. 6.2). Shooting started at 13:30 10.01. with four airguns in operation, a fifth airgun was deployed five hours later. The streamer was deployed for the western part of the profile only. The profile was shot at a speed of 3.7 kn on average, again with a 60 s trigger interval. At 06:00 on 12.01. this was terminated, and instrument recovery started immediately afterwards. Six instruments, that also formed part of the long term seismological network, were not recovered.

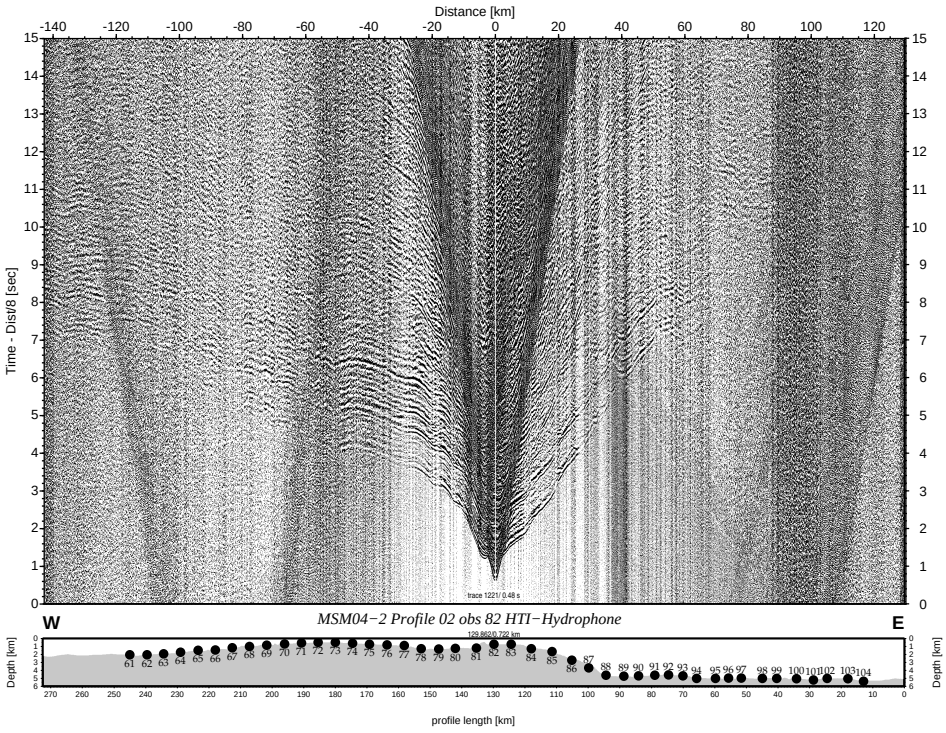

Figure 6.3.2.38: Record section from obs 82 HTI–Hydrophone, Profile 02.

Fig. 6.4: Record Section from OBS 82, Profile 02

6.2.3 Preliminary Interpretation

The wide-angle-reflection refraction profile 01 is a 285 km long line. For this profile, 42 OBH or OBS have been deployed with a spacing of about 5 km. An inversion using the software FAST has been conducted (Figs.6.5 and 6.6).

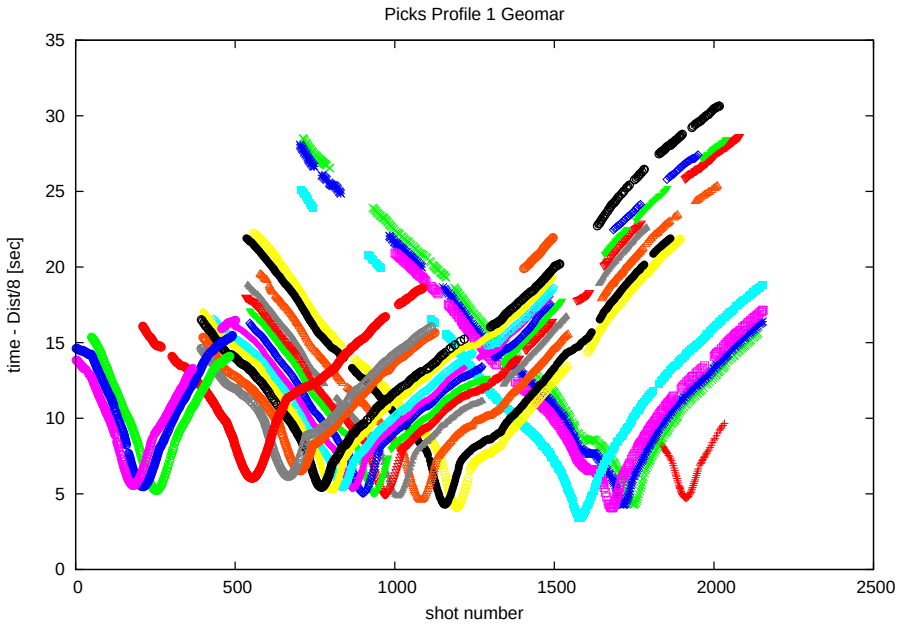

Fig. 6.5: Picks on Profile 01

OBH02, OBS05, OBS08 and OBS11 located on the first western 1/3 part of the profile exhibit refracted waves in the sedimentary layers, then refracted waves through the crust of the Caribbean plate. The arrivals of refracted waves through the crust are affected by the sharp seafloor topography. On the seismic section of OBS 05, for offsets greater than 40 km to the west, Moho reflections have been identified, these Moho reflections are clearly observed on the seismic section of OBS08 for offsets ranging between 40 and 70 km as well as on the seismic section of OBS11 for offsets ranging between 40 and 80 km.

On the seismic section of OBS17, refracted waves through the crust are clearly seen with offsets ranging from 5 to 60 km to the West and Moho reflections from 60 to 100 km. To the West, refracted waves through the crust are seen between km 5 and 60 km offset. Reflected waves are identified from offsets ranging between 40 and 80 km. On the seismic section of OBS22, about 23 km to the east, the Caribbean-Moho reflection (PmP) is identified for offsets greater than 80 km. (reflected waves are also identified from offsets between 20 and 40 km). To the east, reflected waves are clearly identified with a topography effect for offsets ranging between 50 and 80 km. Seismic section of OBS25 shows clear reflected waves on the Moho of the Caribbean plate to the West. The reflected waves between the offsets 35 and 55km are also observed. To the East, reflections are well-identified from offsets ranging from 40 to 65 km.

Seismic section of OBS28 to the West exhibits reflected waves for offsets ranging from 50 to 75km and for offsets ranging from 90 to 155 km. The first ones correspond to reflected waves of the first layers and the latter ones correspond to reflected waves of the Caribbean-Moho discontinuity. The seismic section of OBS29 shows the clearest Caribbean- Moho reflections from offset ranging from 95 km to 160 km.

It seems that the Caribbean-Moho becomes deeper underneath the Island Arc with increasing offsets for the critical reflection.

On the seismic section of OBS33, the first arrivals are more chaotic with diffractions suggesting that we began to sample the accretionary prism. The seismic section of profile 47 shows also some chaotic arrivals with a clear reflected wave from offsets ranging from 35 to 80 km corresponding to the Caribbean Moho reflection. This OBS is the last one on which the Caribbean Moho reflections are observed.

A possible explanation for the vanishing of energy for OBS 36, 38 and 43 could be the exceptional thickness of the accretionary prism in this area.

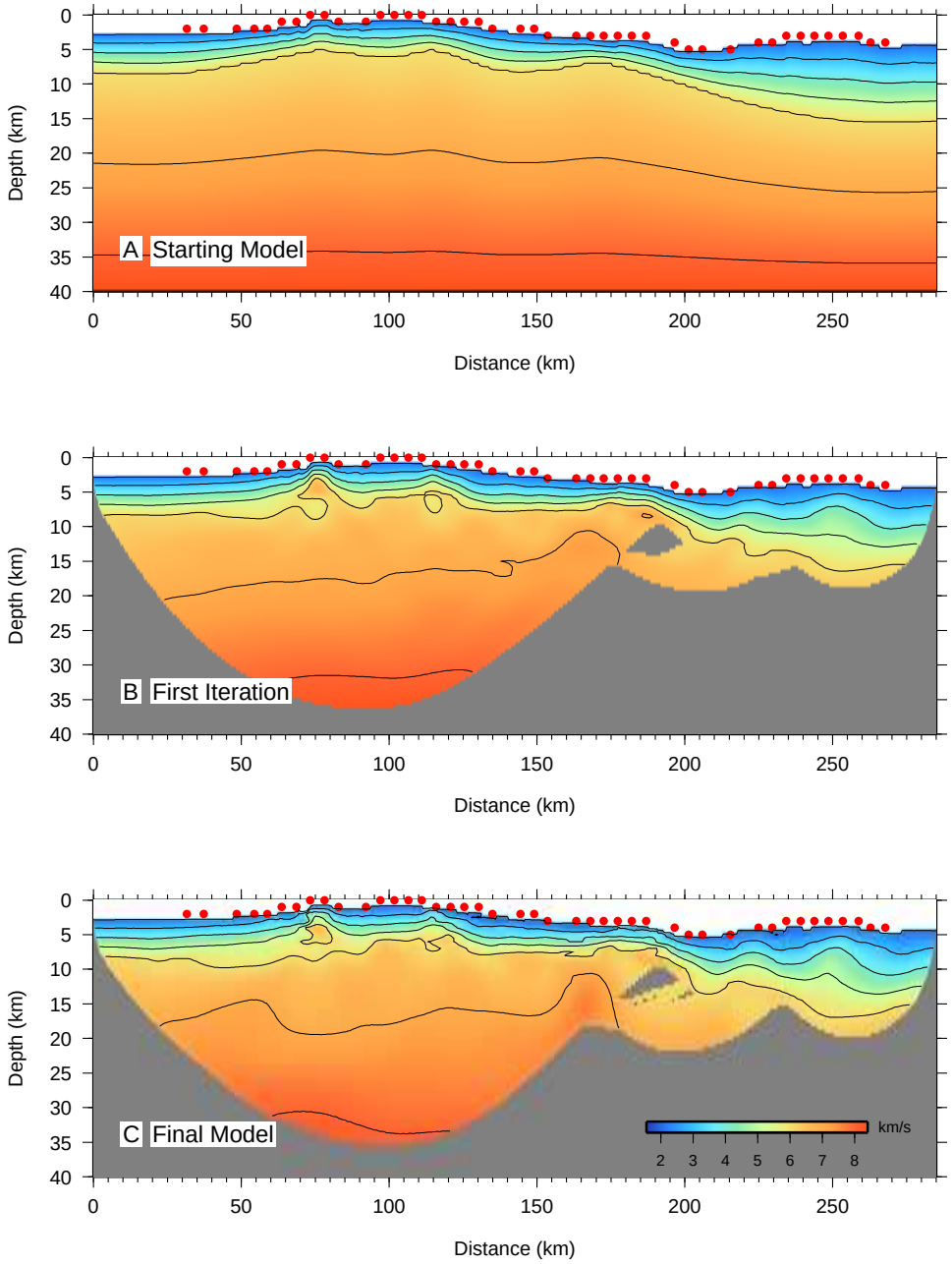

Fig. 6.6: Velocity Model Profile 01, created with FAST by Mikael Evain

6.2.4 Lander

GCPP Deployments on MSM 04/2

Deploy.#	Lat.	Long.	Date	Water Depth mbsl	Deploy. hh:mm	in Sed. Start hh:mm	ex Sed. Stop hh:mm	Rec.on Deck hh:mm	Pore Presssure Measurement	Sed. Recovered [cm]
GCPP-01	15°17,520´ N	60° 30,300´ W	1/7/2007	3040	9:45	11:50	12:05	12:45	NO	367
GCPP-02	15°19,680´ N	60° 25,600´ W	1/7/2007	3380	13:48	15:08	15:23	16:17	NO	100
GCPP-03	15°23,880´ N	60° 16,150´ W	1/7/2007	3568	19:40	20:37	21:00	21:51	NO	179
GCPP-04	15°39,475 ´N	61° 40,172´ W	1/9/2007	1885	12:30	13:00	13:30	14:10	YES	133
GCPP-05	15°43,482´ N	61° 23,950´ W	1/12/2007	955	16:54	17:10	19:10	19:28	YES	0
GCPP-06	16°18,000´ N	60° 17,999´ W	1/13/2007	4875	21:21	22:34	0:35	1:45	YES	174
GCPP-07	16°17,924´ N	60° 17,113´ W	1/14/2007	4950	0:44	2:02	3:02	4:00	YES	267
GCPP-08	16°02,181´ N	60° 49,078´ W	1/16/2007	1023	15:03	15:35	17:34	17:53	YES	0
GCPP-09	16°01,000´ N	60° 50,000´ W	1/16/2007	1062	19:50	20:05	20:25	20:43	YES	0
GCPP-10	14°58,000´ N	60° 23,000´ W	1/17/2007	2685	17:37	18:18	18:48	19:27	YES	380

Coring Results A total of 10 GCPP deployments were carried out during MSM04-2, the first three of which did not correctly measure pore pressure due to a faulty pressure sensor, the remaining 7 measurements were successful, providing high resolution pressure data (sampling rate of 18 samples/sec.).

The length of core recovered varied from 100 to 380cm, depending on the lithology encountered. Three GCPP stations did not recover any sediment, traces of material in the corer showed that the sea floor in these cases

consisted primarily of coarse grained carbonate material.

Lithological overview and lithologs

GCPP-01(see Fig.6.8)

367cm core recovered; silty clay with sandy intercalations, bioturbation, shell fragments, ash particles

GCPP-02(see Fig.6.9)

100cm core recovered; silty clay matrix, shell fragments, sandy spots, dark lenses

GCPP-03(see Fig.6.10)

179cm core recovered; silty clay matrix, shell fragments, lenses containing minerals (Amph, Plag?)

GCPP-04

133cm core recovered; core to be opened in onshore lab for geotechnical testing; cylinder sample (10cc) taken at 0cm, 34cm (2x) and 133cm core depth

GCPP-06

174cm core recovered; core to be opened in onshore lab for geotechnical testing; cylinder sample (10cc) taken at 76cm and 170cm (2x) core depth

GCPP-07

267cm core recovered; core to be opened in onshore lab for geotechnical testing; cylinder sample (10cc) taken at 68cm, 168cm and 260cm core depth

GCPP-10

366cm core recovered; core to be opened in onshore lab for geotechnical testing; cylinder sample (10cc) taken at 364 and 264cm core depth

GCPP-05,08 and 09

no recovery

Results of pore pressure measurements

The 7 differential pore pressure records obtained showed in all cases a similar pattern during lowering and penetration of the GCPP. Typical results are shown using GCPP-07 as an example (Fig.6.7).

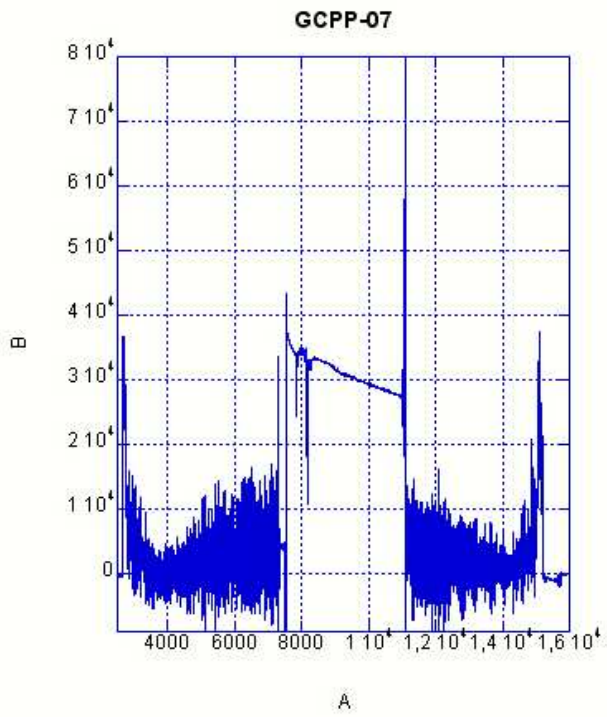

Fig. 6.7: Differential pore pressure vs time (seconds of the day), GCPP-07 test on a deep water mud volcano (4950m).

The differential pressure sensor shows nearly constant values immediately before and after deployment, during descent and ascent of the GCPP pressure values are varying over a broad range of 2000-3000 Pascal. The penetration into the sediment is marked by a pressure peak and slowly decaying differential pressure that is related to in situ sediment permeability.

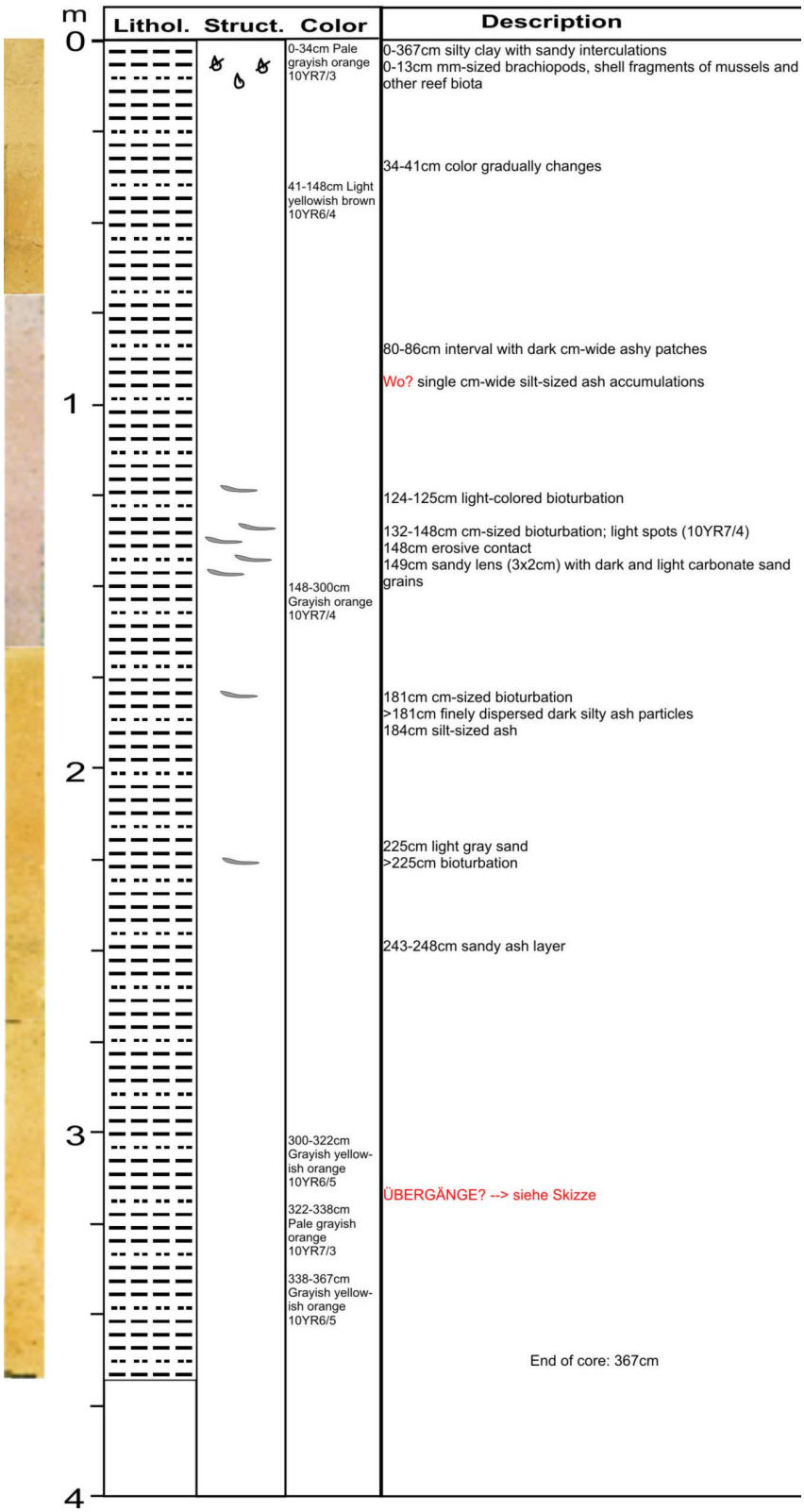

Fig. 6.8: Lithology GCPP-01

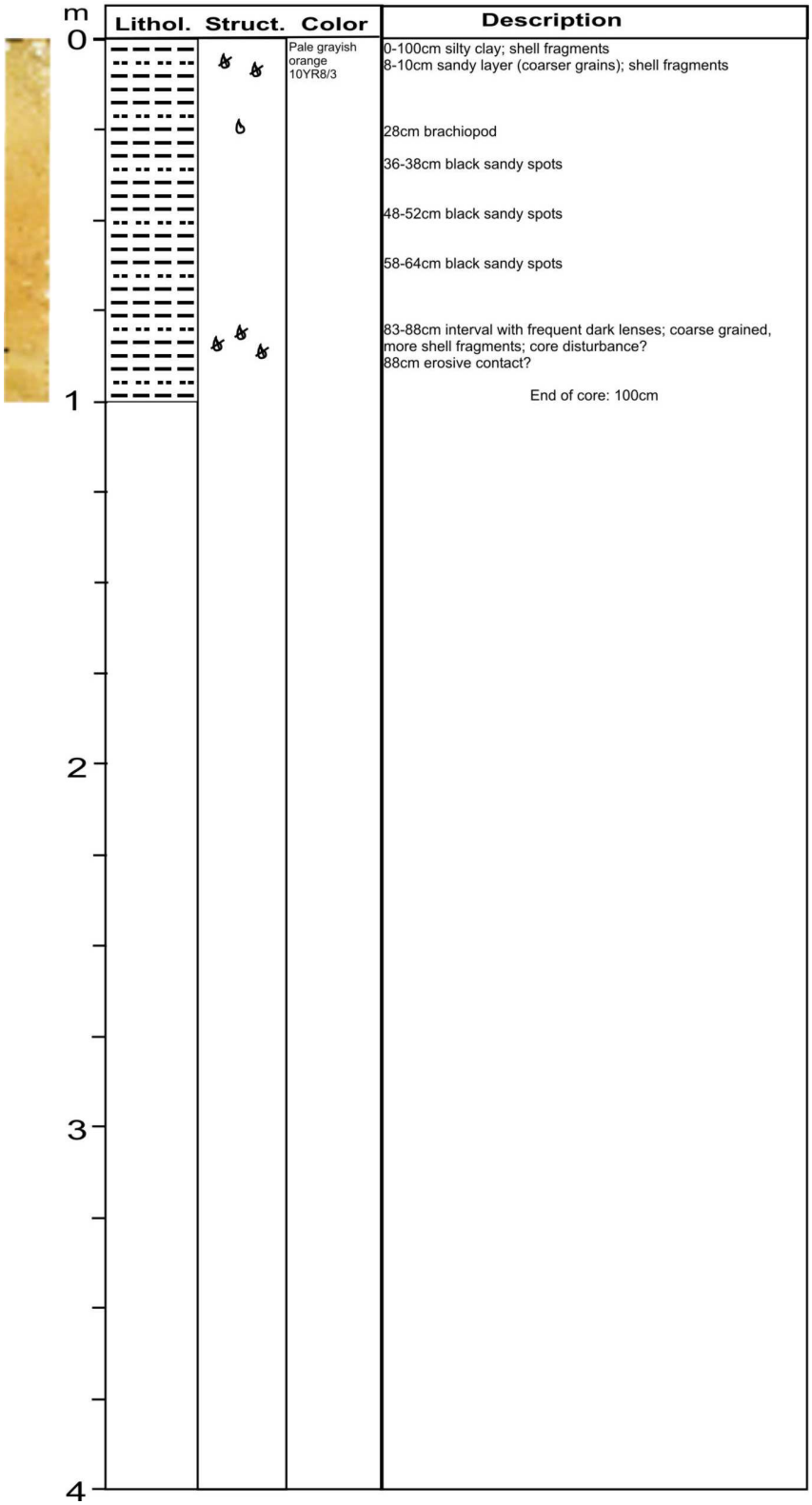

Fig. 6.9: Lithology GCPP-02

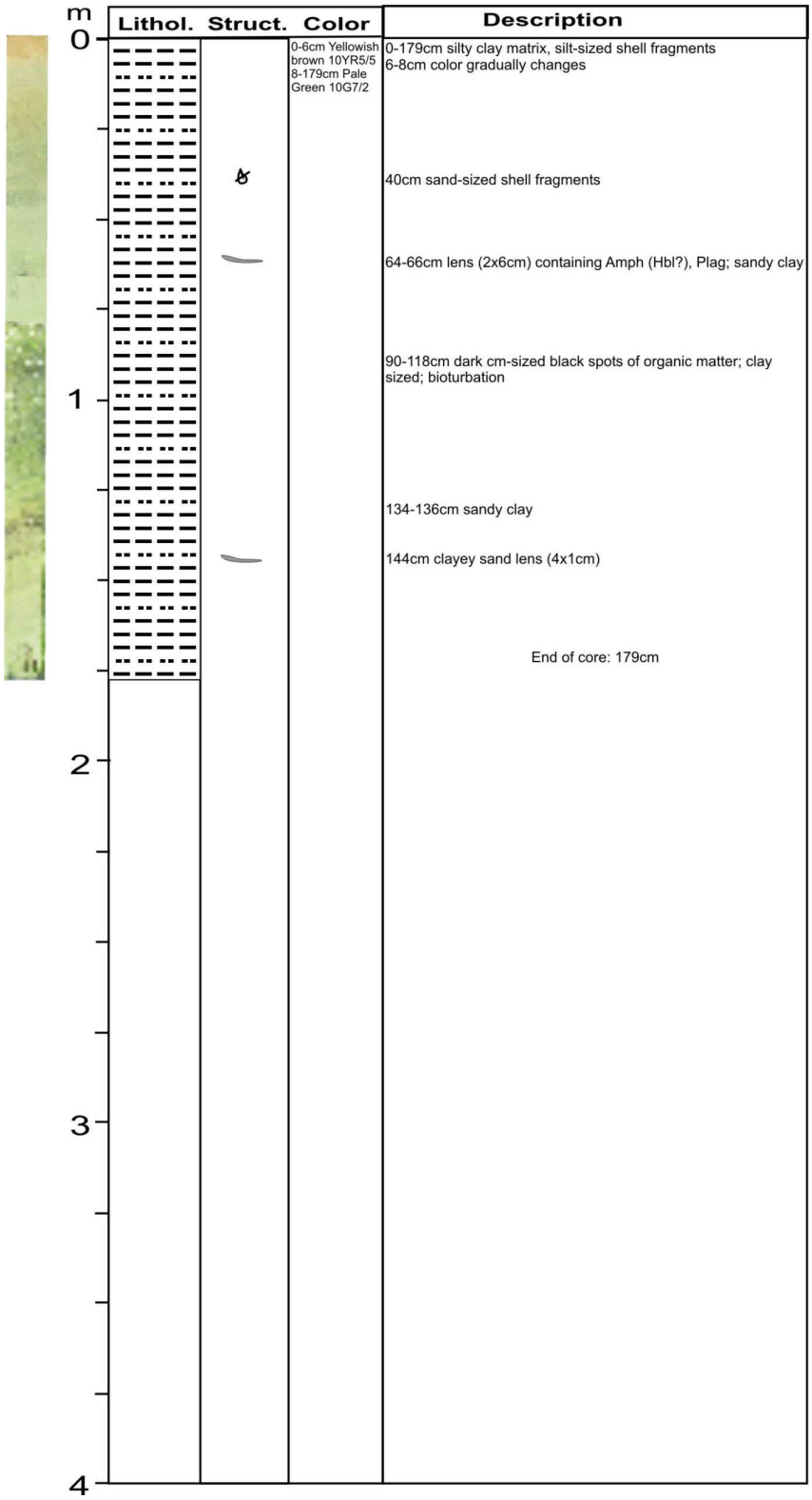

Fig. 6.10: Lithology GCPP-03

A Profile 01

Tab. A.1: Profile 1

station	lat (N) D:M	long (W) D:M	depth (m)	dist to next (Nm)	deploy. date	recov. date	releaser code	ant. chan.	recorder	sensor	skew (ms)
OBH 01	14°50,060	61°32,080	2702	3,1	03.01.2007	06.01.2007	145240	D	MLS 040805	OAS	4
OBH 02	14°51,343	61°29,150	2657	3,1	03.01.2007	06.01.2007	430274	D	MLS 000713	HTI	-3
OBH 03	14°52,655	61°26,233	2550	3,0	03.01.2007	06.01.2007	435610	C	MLS 951258	HTI	21
OBH 04	14°53,926	61°23,447	2457	3,2	03.01.2007	06.01.2007	133770	C	MLS 991242	HTI	0
OBH 05	14°55,266	61°20,433	2236	2,6	03.01.2007	06.01.2007	134123	C	MLS 991236	HTI	-2
OBS 06	14°56,331	61°18,076	2084	2,6	03.01.2007	06.01.2007	133563	D	MLS 040807	HTI + Owen 4,5 Hz	0
OBS 07	14°57,385	61°15,680	1820	2,6	03.01.2007	06.01.2007	143175	D	MLS 010406	HTI + Owen 4,5 Hz	-1
OBS 08	14°58,461	61°13,228	1507	2,6	03.01.2007	06.01.2007	430232	D	MLS 040803	HTI + Owen 4,5 Hz	1
OBS 09	14°59,538	61°10,884	810	2,6	03.01.2007	06.01.2007	145331	C	MLS 020601	HTI + Owen 4,5 Hz	10
OBS 10	15°00,612	61°08,444	502	2,6	03.01.2007	06.01.2007	427260	D	MLS 991244	HTI + Owen 4,5 Hz	2
OBS 11	15°01,696	61°06,067	1091	2,6	03.01.2007	06.01.2007	31139	C	05-09	4,5 Hz	2
OBS 12	15°02,742	61°03,662	1032	2,6	03.01.2007	06.01.2007	29018	A	05-07	4,5 Hz	?
OBS 13	15°03,802	61°01,260	1105	2,6	03.01.2007	06.01.2007	29012	A	05-08	4,5 Hz	3
OBS 14	15°04,873	60°58,858	870	2,6	03.01.2007	06.01.2007	30236	B	06-02	4,5 Hz	5
OBS 15	15°05,968	60°56,454	821	2,6	03.01.2007	06.01.2007	31142	A	06-01	4,5 Hz	20
OBS 16	15°07,025	60°54,035	843	2,6	03.01.2007	06.01.2007	31136	D	05-03	4,5 Hz	13
OBS 17	15°08,033	60°51,744	986	2,6	03.01.2007	06.01.2007	29014	B	05-04	4,5 Hz	12
OBS 18	15°09,117	60°49,259	1239	2,6	03.01.2007	06.01.2007	29010	C	05-05	4,5 Hz	?
OBS 19	15°10,217	60°46,811	1425	2,6	03.01.2007	07.01.2007	29016	A	05-06	4,5 Hz	-12
OBS 20	15°11,257	60°44,461	1619	2,6	03.01.2007	07.01.2007	29011	B	05-10	4,5 Hz	9
OBS 21	15°12,350	60°41,998	1953	2,6	04.01.2007	07.01.2007	133736	C	MLS 040102	HTI + Owen 4,5 Hz	-8
OBS 22	15°13,431	60°39,621	2208	2,6	04.01.2007	07.01.2007	131245	C	MLS 040806	HTI + Owen 4,5 Hz	2
OBS 23	15°14,553	60°37,231	2393	2,6	04.01.2007	07.01.2007	427430	D	MLS 991257	HTI + Owen 4,5 Hz	4
OBS 24	15°15,580	60°34,837	2702	2,6	04.01.2007	07.01.2007	134037	D	MLS 010404	HTI + Owen 4,5 Hz	12
OBH 25	15°16,635	60°32,436	2862	2,6	04.01.2007	07.01.2007	131351	D	MLS 991233	DPG	8
OBS 26	15°17,704	60°30,044	3029	2,6	04.01.2007	07.01.2007	133664	D	MLS 001253	HTI + Owen 4,5 Hz	14
OBS 27	15°18,766	60°27,635	3257	2,6	04.01.2007	07.01.2007	131203	D	MLS 001235	HTI + Owen 4,5 Hz	-4
OBS 28	15°19,854	60°25,249	3392	2,6	04.01.2007	07.01.2007	250177	C	MLS 010408	HTI + Owen 4,5 Hz	-2
OBS 29	15°20,917	60°22,829	3550	2,6	04.01.2007	07.01.2007	435656	C	MLS 991234	HTI + Owen 4,5 Hz	6
OBS 30	15°21,980	60°20,430	3835	2,6	04.01.2007	07.01.2007	427226	C	MLS 010403	HTI + Owen 4,5 Hz	4
OBS 31	15°23,039	60°18,063	3625	2,6	04.01.2007	07.01.2007	131317	A	MLS 991243	HTI + Owen 4,5 Hz	3
OBS 32	15°24,137	60°15,647	3620	2,6	04.01.2007	07.01.2007	427623	C	MLS 040603	HTI + Owen 4,5 Hz	0
OBS 33	15°25,170	60°13,248	3945	2,6	04.01.2007	07.01.2007	427737	D	MLS 050810	HTI + Owen 4,5 Hz	28
OBS 34-D2	15°26,276	60°10,804	4461	2,6	04.01.2007	long-term	31143	B	T4M82	CMG40T	
OBS 44	15°27,323	60°08,425	4917	2,5	04.01.2007	07.01.2007	131415	D	MTS 050816	HTI + Owen 4,5 Hz	1
OBS 45	15°28,400	60°06,030	5165	2,5	04.01.2007	08.01.2007	445070	C	MES 030903	HTI + Owen 4,5 Hz	152
OBS 37-D3	15°29,453	60°03,593	5157	2,5	04.01.2007	long-term	31137	D	06-06	4,5 Hz	
OBS 46	15°30,522	60°01,189	5097	2,5	04.01.2007	08.01.2007	145206	C	MLS 040304	HTI + Owen 4,5 Hz	-4
OBS 47	15°31,598	59°58,808	5092	2,5	04.01.2007	08.01.2007	430067	D	MES 030902	HTI + Owen 4,5 Hz	33
OBS 40-D4	15°32,650	59°56,415	4327	2,5	04.01.2007	long-term	29019	B	T4M80	CMG40T	
OBS 35	15°33,731	59°53,965	4160	2,6	04.01.2007	08.01.2007	31138	C	05-11	4,5 Hz	-2
OBS 36	15°34,789	59°51,639	4231	2,5	04.01.2007	08.01.2007	29009	D	06-12	4,5 Hz	10
OBS 41-D5	15°35,855	59°49,244	3925	2,5	04.01.2007	long-term	31145	A	05-01	4,5 Hz	
OBS 38	15°36,924	59°46,805	3622	2,5	04.01.2007	08.01.2007	29007	D	06-11	4,5 Hz	4
OBS 39	15°37,970	59°44,423	3999	2,5	04.01.2007	08.01.2007	31132	D	06-04	4,5 Hz	-16
OBS 42	15°39,052	59°42,082	3775	2,5	04.01.2007	08.01.2007	31141	B	06-10	4,5 Hz	3
OBS 48	15°40,124	59°39,606	3784	2,5	04.01.2007	08.01.2007	445122	C	MES 031002	HTI + Owen 4,5 Hz	-11
OBS 49	15°41,185	59°37,226	3860	2,5	04.01.2007	08.01.2007	143133	C	MES 030904	HTI + Owen 4,5 Hz	5,8
OBS 50	15°42,264	59°34,836	4266	2,5	04.01.2007	08.01.2007	444760	C	MES 030905	HTI + Owen 4,5 Hz	-13,7
OBS 43	15°43,313	59°32,428	4571		04.01.2007	08.01.2007	31140	D	06-03	4,5 Hz	-8

B Profile 02

Tab. B.1: Profile 2

station	lat (N) D:M	long (W) D:M	depth (m)	dist to next (Nm)	deploy. date	recov. date	releaser code	ant. chan.	recorder	sensor	skew (ms)
OBH 61	15°34,794	61°45,724	2065	2,92	09.01.2007	12.01.2007	134123	D	MLS 040805	HTI	2
OBH 62	15°39,975	61°42,943	2030	2,93	09.01.2007	12.01.2007	133770	C	MLS 000713	HTI	-2
OBS 63	15°37,181	61°40,191	1905	2,93	09.01.2007	12.01.2007	444760	D	MES 030902	HTI + Owen 4,5 Hz	15,8
OBS 64	15°38,365	61°37,468	1734	2,93	09.01.2007	12.01.2007	143133	C	MES 030905	HTI + Owen 4,5 Hz	-7,7
OBS 65	15°39,598	61°34,659	1462	2,93	09.01.2007	12.01.2007	445122	C	MES 030903	HTI + Owen 4,5 Hz	121,1
OBS 66	15°40,798	61°31,855	1400	2,93	09.01.2007	12.01.2007	427226	D	MES 030904	HTI + Owen 4,5 Hz	6,3
OBS 67	15°41,992	61°29,112	1157	2,93	09.01.2007	12.01.2007	131203	C	MES 031002	HTI + Owen 4,5 Hz	3,7
OBS 68	15°43,210	61°26,30	282	2,93	09.01.2007	12.01.2007	250177	D	MLS 991258	HTI + Owen 4,5 Hz	18
OBS 69	15°44,416	61°23,515	826	2,93	09.01.2007	12.01.2007	435656	D	MLS 010408	HTI + Owen 4,5 Hz	-3
OBS 70	15°45,625	61°20,729	672	2,93	09.01.2007	12.01.2007	131317	C	MLS 010403	HTI + Owen 4,5 Hz	4
OBS 71	15°46,812	61°17,937	567	2,92	09.01.2007	13.01.2007	145206	C	MLS 040806	HTI + Owen 4,5 Hz	-627
OBS 72	15°47,951	61°15,213	477	2,92	09.01.2007	13.01.2007	430067	C	MLS 020601	HTI + Owen 4,5 Hz	12
OBS 73	15°49,183	61°12,449	487	2,92	10.01.2007	13.01.2007	427623	D	MLS 991253	HTI + Owen 4,5 Hz	10
OBS 74	15°50,382	61°09,712	600	2,92	10.01.2007	13.01.2007	427737	D	MTS 050810	HTI + Owen 4,5 Hz	6,2
OBS 75	15°51,592	61°06,928	697	2,92	09.01.2007	13.01.2007	433715	D	06-01	4,5 Hz	-13
OBS 76	15°52,824	61°04,143	810	2,92	09.01.2007	13.01.2007	231754	D	05-08	4,5 Hz	n.d.
OBS 77	15°54,030	61°01,316	908	2,92	09.01.2007	13.01.2007	433601	C	05-05	4,5 Hz	-3
OBS 78	15°55,190	60°58,590	1291	2,92	09.01.2007	13.01.2007	433753	B	06-12	4,5 Hz	4
OBS 79	15°56,402	60°55,814	1306	2,80	09.01.2007	13.01.2007	231625	D	05-11	4,5 Hz	7
OBS 80	15°57,619	60°53,177	1233	3,64	09.01.2007	13.01.2007	253223	C	06-02	4,5 Hz	-17
OBS 81-G0	15°59,141	60°49,793	982	3,17	10.01.2007	long-term	445225	B	MCS 060746	HTI + CMG	
OBS 82	16°00,367	60°46,739	744	2,83	10.01.2007	13.01.2007	133664	D	MLS 991243	HTI + Owen 4,5 Hz	-17,5
OBS 83	16°01,506	60°44,048	724	2,83	10.01.2007	13.01.2007	134037	A	MLS 991234	HTI + Owen 4,5 Hz	2
OBS 84-G1	16°02,581	60°41,321	1054	4,18	10.01.2007	long-term	444632	D	MCS 060710	HTI + CMG	
OBS 85	16°03,992	60°37,234	1643	3,38	10.01.2007	13.01.2007	427430	C	MTS 050816	HTI + Owen 4,5 Hz	0
OBS 86	16°05,305	60°34,008	2772	3,23	10.01.2007	13.01.2007	131245	C	MLS 040603	HTI + Owen 4,5 Hz	0
OBS 87-G2	16°06,553	60°30,920	3754	2,73	10.01.2007	long-term	444573	B	MCS 060716	HTI + CMG	
OBS 88	16°07,872	60°28,420	4674	3,02	10.01.2007	13.01.2007	133736	D	MLS 040102	HTI + Owen 4,5 Hz	-7
OBH 89	16°09,043	60°25,517	4719	2,64	10.01.2007	13.01.2007	131351	D	MLS 991233	DPG	9
OBS 90-G3	16°10,080	60°22,986	4723	2,55	10.01.2007	long-term	444674	B	MCS 060714	HTI + CMG	
OBS 91	16°11,326	60°20,636	4582	2,41	10.01.2007	13.01.2007	427260	D	MLS 991244	HTI + Owen 4,5 Hz	2
OBS 92	16°12,264	60°18,340	4606	2,02	10.01.2007	13.01.2007	145331	C	MLS 991257	HTI + Owen 4,5 Hz	-127
OBS 93-G4	16°13,092	60°16,400	4615	2,68	10.01.2007	long-term	445036	D	MCS 060708	HTI + CMG	
OBS 94	16°14,209	60°13,834	4979	3,25	10.01.2007	14.01.2007	430232	D	MLS 040602	HTI + Owen 4,5 Hz	-2
OBS 95	16°15,517	60°10,770	5006	2,30	10.01.2007	14.01.2007	143175	C	MLS 010404	HTI + Owen 4,5 Hz	14
OBS 96-G5	16°16,472	60°08,578	5091	2,13	10.01.2007	long-term	444535	D	MCS 060732	HTI + CMG	
OBS 97	16°17,299	60°06,322	4915	3,70	10.01.2007	14.01.2007	133563	C	MLS 040803	HTI + Owen 4,5 Hz	1
OBS 98	16°19,002	60°03,095	4974	2,32	10.01.2007	14.01.2007	131415	C	MLS 040304	HTI + Owen 4,5 Hz	-4
OBH 99	16°19,761	60°00,812	4951	3,53	10.01.2007	14.01.2007	435610	C	MLS 010406	OAS	2
OBH 100	16°21,7	59°56,6	5074	2,92	10.01.2007	14.01.2007	430274	D	MLS 991242	HTI	0
OBH 101	16°22,596	59°54,848	5192	2,16	10.01.2007	14.01.2007	145240	C	MLS 991236	HTI	-1
OBS 102	16°23,419	59°52,800	5008	3,68	10.01.2007	14.01.2007	445070	C	MLS 040807	HTI + Owen 4,5 Hz	1
OBH 103	16°24,988	50°49,283	5069	2,92	10.01.2007	14.01.2007	3679	A	MLS 060737	HTI	6,1
OBS 104	16°26,162	59°46,564	5321		10.01.2007	14.01.2007	253124	C	06-10	4,5 Hz	6

C Seismology

Tab. C.1: Seismology

station	lat (N) D:M	long (W) D:M	depth (m)	deploy. date	releaser code	ant. chan.	recorder	sensor
OBS 34-D2	15°26,276	60°10,804	4461	04.01.2007	31143	B	T4M82	CMG40T
OBS 37-D3	15°29,453	60°03,593	5157	04.01.2007	31137	D	06-06	4,5 Hz
OBS 40-D4	15°32,650	59°56,415	4327	04.01.2007	29019	B	T4M80	CMG40T
OBS 41-D5	15°35,855	59°49,244	3925	04.01.2007	31145	A	05-01	4,5 Hz
OBS 53-B5	15°11,895	59°35,395	3848	08.01.2007	29010	C	06-04	4,5 Hz
OBS 52-B4	15°08,619	59°42,571	4025	08.01.2007	29016	A	T4M98	CMG40T
OBS 113-B3	15°05,377	59°49,990	4657	17.01.2007	29018	C	06-03	4,5 Hz
OBS 54-C5	15°25,749	59°42,539	3669	08.01.2007	29014	B	T4L84	CMG40T
OBS 51-C4	15°22,198	59°49,970	4378	08.01.2007	29011	B	T4M99	CMG40T
OBS 123-C3	15°18,941	59°56,936	5163	17.01.2007	30235	C	06-12	4,5 Hz
OBS 55-E5	15°49,309	59°54,398	4281	09.01.2007	31136	D	T4M97	CMG40T
OBS 56-E4	15°45,923	60°02,420	4256	09.01.2007	31142	A	05-07	4,5 Hz
OBS 57-E3	15°42,802	60°08,843	4796	09.01.2007	30236	B	T4L52	CMG40T
OBS 58-E2	15°39,150	60°17,045	5078	09.01.2007	29012	A	05-09	4,5 Hz
OBS 59-E1	15°34,287	60°27,965	3035	09.01.2007	31139	C	T4M83	CMG40T
OBS 156-F6	16°03,142	59°51,893	4581	17.01.2007	31128	A	T4N00	CMG40T
OBS 155-F5	15°59,619	59°59,768	4401	16.01.2007	31140	D	06-02	4,5 Hz
OBS 154-F4	15°56,158	60°07,725	3815	16.01.2007	31141	B	T4L85	CMG40T
OBS 153-F3	15°53,169	60°14,361	3822	16.01.2007	29009	D	05-11	4,5 Hz
OBS 152-F2	15°49,658	60°22,103	4222	16.01.2007	31138	C	06-01	4,5 Hz
OBS 151-F1	15°44,729	60°33,138	1926	16.01.2007	29007	D	T4L53	CMG40T
OBS 60-F0	15°40,743	60°44,413	2108	09.01.2007	31132	D	05-04	4,5 Hz
OBS 81-G0	15°59,141	60°49,793	982	10.01.2007	445225	B	MCS 060746	HTI + CMG
OBS 84-G1	16°02,581	60°41,321	1054	10.01.2007	444632	D	MCS 060710	HTI + CMG
OBS 87-G2	16°06,553	60°30,920	3754	10.01.2007	444573	B	MCS 060716	HTI + CMG
OBS 90-G3	16°10,080	60°22,986	4723	10.01.2007	444674	B	MCS 060714	HTI + CMG
OBS 93-G4	16°13,092	60°16,400	4615	10.01.2007	445036	D	MCS 060708	HTI + CMG
OBS 96-G5	16°16,472	60°08,578	5091	10.01.2007	444535	D	MCS 060732	HTI + CMG
OBS 105-G6	16°19,760	60°00,878	4965	14.01.2007	427430	A	MLS 991234	HTI + Owen 4,5 Hz
OBS 106-G7	16°23,475	59°52,805	5011	14.01.2007	145206	C	MLS 991243	HTI + Owen 4,5 Hz
OBS 107-H7	16°35,562	59°58,936	5805	14.01.2007	430067	D	MLS 040807	HTI + Owen 4,5 Hz
OBS 108-H6	16°31,944	60°06,988	5437	14.01.2007	131351	D	MLS 991236	HTI + Owen 4,5 Hz
OBS 109-H5	16°28,626	60°14,748	5406	14.01.2007	444760	B	MCS 060709	HTI + CMG
OBS 110-H4	16°25,060	60°22,552	5199	15.01.2007	445122	B	MCS 060745	HTI + CMG
OBS 111-I4	16°40,644	60°30,640	5270	15.01.2007	143133	C	MLS 991244	DPG + Webb
OBS 112-I5	16°43,797	60°22,959	4942	15.01.2007	427226	C	MLS 040102	HTI + Owen 4,5 Hz
OBS 113-I6	16°47,115	60°15,042	4847	15.01.2007	427623	C	MLS 000713	HTI + Owen 4,5 Hz
OBS 114-I7	16°50,382	60°06,474	5153	15.01.2007	131203	C	MLS 010408	HTI + Owen 4,5 Hz
OBS 115-K7	17°14,098	60°18,804	4836	15.01.2007	435656	C	MLS 010404	HTI + Owen 4,5 Hz
OBS 116-L5	17°16,982	60°40,585	4786	15.01.2007	131245	C	MLS 991257	HTI + Owen 4,5 Hz
OBS 117-K5	17°06,666	60°34,784	5120	15.01.2007	250177	D	MLS 040803	HTI + Owen 4,5 Hz
OBS 118-J4	16°52,212	60°36,043	5435	15.01.2007	133664	C	MLS 010410	DPG + Webb
OBS 119-J3	16°49,092	60°43,095	5482	15.01.2007	427737	C	MLS 991253	HTI + Owen 4,5 Hz
OBS 120-K3	17°00,046	60°48,758	5617	15.01.2007	134123	D	MLS 040805	DPG + Webb
OBS 121-K2	16°56,438	60°56,228	4912	15.01.2007	133563	C	MLS 991258	HTI + Owen 4,5 Hz
OBS 122-K1	16°53,914	61°04,913	2473	15.01.2007	145331	D	MLS 010403	HTI + Owen 4,5 Hz
OBS 123-J1	16°41,691	61°01,621	4705	15.01.2007	427260	D	MLS 991242	HTI + Owen 4,5 Hz
OBS 124-I2	16°34,689	60°45,150	5754	16.01.2007	145240	D	MLS 010410	DPG + Webb
OBS 125-H-1	16°08,027	61°03,350	456	16.01.2007	430274	D	MLS 040806	HTI + Owen 4,5 Hz
OBS 126-H0	16°12,579	60°53,419	572	16.01.2007	131317	D	MLS 040603	HTI + Owen 4,5 Hz
OBS 127-H1	16°15,845	60°44,926	912	16.01.2007	445070	A	MCS 060737	HTI + CMG
OBS 128-H2	16°18,840	60°36,838	2769	16.01.2007	445164	A	MCS 060717	HTI + CMG

D Airguns on Profiles

MSM 04-02 Martinique - Profile 1 course 267,1°

date	time (UTC)	lat (N) D:M	long (W) D:M	depth (m)	guns	trigger interval	shot number	profile length (Nm)	comments
04.01.2007	22:18	15°48,968	59°23,898	4470,1	5 guns green	40 s	1	0,00	first shot
04.01.2007	22:49	15°47,620	59°25,001	4418,7	5 guns green	40 s	48	2,41	
04.01.2007	22:50	15°47,500	59°25,043	4421,4	5 guns green	60 s	49	2,47	
05.01.2007	02:37	15°39,458	59°41,001	3847,6	guns 4 and 5 yellow	60 s	276-283	19,58	amplitude of noise before the pulse is higher than pulse
05.01.2007	02:45	15°39,223	59°41,535	3865,4	gun 4 set to blue, gun 5 yellow	60 s	284	20,16	parameters tested
05.01.2007	04:14	15°36,637	59°47,382	3855,6	gun 4 blue, gun 5 yellow	60 s	373-401	26,56	gun 5 tried to set to manual, but stays yellow
05.01.2007	06:21	15°33,061	59°55,441	4364,1	gun 4 blue, gun 5 yellow	60 s	500	35,37	gun 3 sometimes yellow
06.01.2007	09:59	14°42,967	61°48,110	2810,7	gun 4 blue, gun 5 yellow	60 s	2156	158,68	last shot

MSM 04-02 Martinique - Profile 2 course 253,9°

date	time (UTC)	lat (N) D:M	long (W) D:M	depth (m)	guns	trigger interval	shot number	profile length (Nm)	comments
10.01.2007	17:28	16°29,733	59°40,688	5007,8	guns 1 to 3 green, gun 4 blue, gun 5 red	30 s	1	0,00	first shot
10.01.2007	17:31	16°29,602	59°40,868	5089,2	guns 1 to 3 green, gun 4 blue, gun 5 red	30 s	7	0,22	
10.01.2007	17:31	16°29,580	59°40,898	5096,3	guns 1 to 3 green, gun 4 blue, gun 5 red	40 s	8	0,26	
10.01.2007	17:34	16°29,485	59°41,028	5095,1	guns 1 to 3 and 5 green	40 s	12	0,42	gun 4 dead
10.01.2007	17:41	16°29,220	59°41,417	5068,9	guns 1 to 3 and 5 green	40 s	23	0,89	
10.01.2007	17:42	16°29,196	59°41,450	5039,9	guns 1 to 3 and 5 green	60 s	24	0,93	
10.01.2007	19:54	16°24,841	59°49,640	5036,2	guns 1 to 3 and 5 green	60 s	157	10,21	gun 5 occasionally red (due to weak signal from sensor)
10.01.2007	23:03	16°20,280	60°00,239	4928,1	guns 1 to 3 green, gun 5 sometimes red	60 s	346	21,75	gun 4 redeployed
10.01.2007	23:14	16°20,030	60°00,829	4985,7	all 5 guns shooting normally	60 s	357	22,39	gun 5 occasionally red (due to weak signal from sensor)
12.01.2007	09:27	15°29,617	61°51,803	2188	guns 1 to 3 and 5 green	60 s	2408	144,28	gun 4 off
12.01.2007	09:40	15°29,309	61°58,562	2260,9	guns 1 to 3 green	60 s	2421	151,04	gun 5 off
12.01.2007	10:03	15°28,769	61°59,820	2240,8	guns 1 to 3 green	60 s	2444	152,41	last shot

green: normal fire
yellow: out of range
red: no sensor signal detected
blue: manual tuning

Bibliography

[1] Generation of high pore pressure in accretionary prisms: Inferences from the Barbados subduction complex. *Journal of Geophysical Research*, 93:8893–8910, August 1988.

[2] Abt, D. L., Fischer, K. M., Martin, L., Abers, G. A., Protti, J. M., Gonzalez, V., and Strauch, W. Shear-wave Splitting Tomography in the Central American Subduction Zone: Implications for Flow and Melt in the Mantle Wedge. *AGU Fall Meeting Abstracts*, pages C5+, December 2006.

[3] Adamek, S., Frohlich, C., and Pennington, W. D. Seismicity of the Caribbean-Nazca boundary: Constraints on microplate tectonics of the Panama region. *Journal of Geophysical Research*, 93:2053–2075, March 1988.

[4] Aguiar, A. C., Melbourne, T. I., and Scrivner, C. W. Automated Tremor Analysis From the Cascadia Subduction Zone. *AGU Fall Meeting Abstracts*, pages A1536+, December 2006.

[5] Antignano, A. and Manning, C. E. Rutile Solubility in Supercritical Albite-H2O fluids: Implications for Element Mobility in Subduction Zones. *AGU Fall Meeting Abstracts*, pages C1089+, December 2006.

[6] Aung, T. T., Okamura, Y., Satake, K., Swe, W., Swe, T. L., Saw, H., and Tun, S. T. Search For Paleoseismolgical Evidences Of Subduction-zone Earthquakes Along The Northwestern (Rakhine) Coast Of Myanmar. *AGU Fall Meeting Abstracts*, pages F5+, December 2006.

[7] Babist, J., Handy, M. R., Konrad-Schmolke, M., and Hammerschmidt, K. Precollisional, multistage exhumation of subducted continental crust: The Sesia Zone, western Alps. *Tectonics*, 25:C6008+, December 2006.

[8] Bangs, N. L., Christeson, G. L., and Shipley, T. H. Structure of the Lesser Antilles subduction zone backstop and its role in a large accretionary system. *Journal of Geophysical Research (Solid Earth)*, 108:6–1, July 2003.

[9] Bangs, N. L., Shipley, T. H., and Moore, G. F. Elevated fluid pressure and fault zone dilation inferred from seismic models of the northern Barbados Ridge decollement. *Journal of Geophysical Research*, 101:627–642, 1996.

[10] Bangs, N. L. B. and Westbrook, G. K. Seismic modeling of the decollement zone at the base of the Barbados Ridge accretionary complex. *Journal of Geophysical Research*, 96:3853–3866, March 1991.

[11] Bannister, S., Toulmin, S., Henrys, S., Reyners, M., Barker, D., Pecher, I., Sutherland, R., Uruski, C., and Maslen, G. Imaging the Subduction Decollement, Hikurangi Subduction Zone, New Zealand. *AGU Fall Meeting Abstracts*, pages A394+, December 2006.

[12] Barckhausen, U. The Segmentation of the Subduction Zone Offshore Sumatra: Relations Between Upper and Lower Plate. *AGU Fall Meeting Abstracts*, pages A29+, December 2006.

[13] Bernard, P. and Lambert, J. Subduction and seismic hazard in the Northern Lesser Antilles: Revision of historical seismicity. *Bulletin of the Seismological Society of America*, 78:1965–1983, 1988.

[14] Bogdanov, I., Genthon, P., Thovert, J., and Adler, P. M. Fracturation Pattern in the Limestone Loyaute Islands and its Relation to the Neighbouring Vanuatu Subduction Zone (SW PAcific). *AGU Fall Meeting Abstracts*, pages D533+, December 2006.

[15] Boria, R. I. and Dreiss, S. J. Numerical modeling of accretionary wedge mechanics: Application to the Barbados subduction problem. *Journal of Geophysical Research*, 94:9323–9339, July 1989.

[16] Bouysse, P. Opening of the Grenada back-arc basin and evolution of the Caribbean Plate during the Mesozoic and early Paleogene. *Tectonophysics*, 149:121–143, 1988.

[17] Bouysse, P. and Westercamp, D. Subduction of Atlantic aseismic ridges and Late Cenozoic evolution of the Lesser Antilles island arc. *Tectonophysics*, 175:349–380, 1990.

[18] Bowin, C. *Caribbean gravity field and plate tectonics.* Boulder, Colo.: Geological Society of America, 1976.

[19] Brueckmann, W., Hayward, N., Hunze, S., Tobin, H., and Scientific Party Leg 196. From Protodecollement to Incipient Plate Boundary - Physical Property Characteristics of Nankai and Barbados Decollement Zones Compared. *AGU Fall Meeting Abstracts*, pages A849+, December 2001.

[20] Brueckmann, W., Hunze, S., and Leg 196, O. Logging While Drilling In The Frontal Part of The Nankai and Barbados Accretionary Prisms - Physical Characteristics of The Decollement Zone Compared Revealed. *EGS XXVII General Assembly, Nice, 21-26 April 2002, abstract #5436*, 27:5436–+, 2002.

[21] Burlini, L., di Toro, G., Meredith, P., Mainprice, D., and Burg, J. Seismic tremor under the subduction zones: the rock-physics interpretation. *AGU Fall Meeting Abstracts*, pages A7+, December 2006.

[22] Chase, R. L. and Bunce, E. T. Underthrusting of the Eastern Margin of the Antilles by the Floor of the Western North Atlantic Ocean, and Origin of the Barbados Ridge. *Journal of Geophysical Research*, 74:1413–+, March 1969.

[23] Chen, W., Brudzinski, M. R., and Green, H. W. Thermo-Petrologic Evolution of Subducted Lithosphere in the Transition Zone. *AGU Fall Meeting Abstracts*, pages A2+, December 2006.

[24] Cheng, W. Tomographic imaging of the convergent zone in eastern Taiwan : a subducting forearc sliver revealed? *AGU Fall Meeting Abstracts*, pages A397+, December 2006.

[25] Chlieh, M., Avouac, J., Sieh, K., and Natawidjaja, D. H. Sources characteristics and Afterslip of Great Earthquakes in the Western Sunda Subduction Zone. *AGU Fall Meeting Abstracts*, pages B1+, December 2006.

[26] Christeson, G. L., Bangs, N. L., and Shipley, T. H. Deep structure of an island arc backstop, Lesser Antilles subduction zone. *Journal of Geophysical Research (Solid Earth)*, 108:2–1, July 2003.

[27] Cox, C. et al. A Deep-Sea Differential Pressure Gauge. *J. of Atmospheric and Oceanic Tech.*, 1:237–246, 1984.

[28] Cross, R. S. and Freymueller, J. T. Plate coupling variation and block translation in the Andreanof segment of the Aleutian arc determined by subduction zone modeling using GPS data. *Geophysical Research Letters*, 34:6304–+, March 2007.

[29] Cruz Gómez, R. C. and Bulgakov, S. N. Remote sensing observations of the coherent and non-coherent ring structures in the vicinity of Lesser Antilles. *Annales Geophysicae*, 25:331–340, March 2007.

[30] Daniel, I., Koga, K. T., Reynard, B., Petitgirard, S., Chollet, M., and Simionovici, A. Partitioning of Trace Elements Between Hydrous Minerals and Aqueous Fluids : a Contribution to the Chemical Budget of Subduction Zones. *AGU Fall Meeting Abstracts*, pages D4+, December 2006.

[31] Davidson, J. P. Isotopic and trace element constraints on the petrogenesis of subduction-related lavas from martinique, lesser antilles. *Journal of Geophysical Research*, 91:5943–5962, May 1986.

[32] Delahaye, E. J., Townend, J., Reyners, M. E., and Chadwick, M. P. Seismic Tremor and Small Earthquakes Associated With Slow Slip in the Hikurangi Subduction Zone, New Zealand. *AGU Fall Meeting Abstracts*, pages A1548+, December 2006.

[33] Demets, C., Jansma, P. E., Mattioli, G. S., Dixon, T. H., Farina, F., Bilham, R., Calais, E., and Mann, P. GPS geodetic constraints on Caribbean-North America plate motion. *Geophysical Research Letters*, 27:437–+, 2000.

[34] Deng, J. and Sykes, L. R. Determination of Euler pole for contemporary relative motion of Caribbean and North American plates using slip vectors of interplate earthquakes. *Tectonics*, 14:39–53, 1995.

[35] Dixon, T. H., Farina, F., DeMets, C., Jansma, P., Mann, P., and Calais, E. Relative motion between the Caribbean and North American plates and related boundary zone deformation from a decade of GPS observations. *Journal of Geophysical Research*, 103:15157–15182, July 1998.

[36] Dorel, J. Seismicity and seismic gap in the Lesser Antilles arc and earthquake hazard in Guadeloupe. *Geophysical Journal International*, 67:679–695, 1981.

[37] Duke, G. I. N40W Alkalic Trend From Black Hills to Alberta May Correspond to Presence of Subducted Slab Edge at Transition Zone at 49-50 Ma. *AGU Fall Meeting Abstracts*, pages D613+, December 2006.

[38] Dziewonski, A. M., Ekström, G., and Maternovskaya, N. N. Centroid-moment tensor solutions for April-June, 1999. *Physics of the Earth and Planetary Interiors*, 119:161–171, May 2000.

[39] Eberhart-Phillips, D., Reyners, M., Chadwick, M., and Stuart, G. 3-D Distribution of Anisotropy and Attenuation in the Hikurangi Subduction Zone, New Zealand. *AGU Fall Meeting Abstracts*, pages G2+, December 2006.

[40] Ernst, W. G., Tsujimori, T., Zhang, R., and Liou, J. G. Permo-Triassic Collision, Subduction-Zone Metamorphism, and Tectonic Exhumation Along the East Asian Continental Margin. *AGU Fall Meeting Abstracts*, pages B6+, December 2006.

[41] Faul, U., Wiens, D., and Conder, J. Comparison of Forward Calculated Velocity Structure With Tomographic Images of Subduction Zones. *AGU Fall Meeting Abstracts*, pages G1+, December 2006.

[42] Fehn, U., Lu, Z., Hensen, C., Wallmann, K., and Snyder, G. T. Fluid Flow in Subduction Zones: Comparison of I-129 Results From the Main and Fore Arc of Central America. *AGU Fall Meeting Abstracts*, pages B1731+, December 2006.

[43] Feuillard, M. Macrosismicite de la Guadeloupe et de la Martinque. *report, Inst. de Phys. du Globe de Paris*, 1985.

[44] Feuillet, N., Manighetti, I., Tapponnier, P., and Jacques, E. Arc parallel extension and localization of volcanic complexes in Guadeloupe, Lesser Antilles. *Journal of Geophysical Research (Solid Earth)*, 107:3–1, December 2002.

[45] Feuillet, N., Tapponnier, P., Manighetti, I., Villemant, B., and King, G. C. P. Differential uplift and tilt of Pleistocene reef platforms and Quaternary slip rate on the Morne-Piton normal fault (Guadeloupe, French West Indies). *Journal of Geophysical Research (Solid Earth)*, 109:2404–+, February 2004.

[46] Fleitout, L. and Krien, Y. Subducted slabs and plate dynamics forces: constraints from gravity data above subduction zones. *AGU Fall Meeting Abstracts*, pages D1639+, December 2006.

[47] Flinch, J. F. et al. Structure of the Gulf of Paria pull-apart Basin (Eastern Venezuela-Trinidad). *In: P. Mann (Editor), Caribbean Basins. Sedimentary Basins of the World*, pages 477–494, 1999.

[48] Flueh, E. R. and Bialas, J. A digital, high data capacity ocean bottom recorder for seismic investigations. *Int. Underwater Systems Design*, 18(3):18–20, 1996.

[49] Flueh, E. R. and Bialas, J. Ocean Bottom Seismometers. *Sea Technology*, 40(4):41–46, 1999.

[50] Franke, D., Gaedicke, C., Ladage, S., Tappin, D., Neben, S., Ehrhardt, A., Mueller, C., and Djajadihardja, Y. Contrasting styles of deformation along the Sumatra subduction zone. *AGU Fall Meeting Abstracts*, pages A17+, December 2006.

[51] Gao, H. and Schmidt, D. A. The Slip History of the 2004 Slow Slip Event on the Northern Cascadia Subduction Zone. *AGU Fall Meeting Abstracts*, pages A1540+, December 2006.

[52] Geist, E. L. Diversity of tsunamigenic earthquakes along the Sunda subduction zone: 2004- 2006. *AGU Fall Meeting Abstracts*, pages C1+, December 2006.

[53] Greve, S. M. and Savage, M. K. Strong Variations in Seismic Anisotropy Across a Mantle Wedge, Hikurangi Subduction Zone, New Zealand. *AGU Fall Meeting Abstracts*, pages C511+, December 2006.

[54] Gross, K., Buske, S., and Wigger, P. Reflection Seismic Imaging of the Subduction Zone in Southern Central Chile (Project TIPTEQ). *AGU Fall Meeting Abstracts*, pages D459+, December 2006.

[55] Grove, T. L., Chatterjee, N., Medard, E., and Parman, S. W. Chlorite Stability in the Mantle Wedge and its Role in Subduction Zone Melting Processes. *AGU Fall Meeting Abstracts*, pages A2+, December 2006.

[56] Haberland, C., Rietbrock, A., Lange, D., Bataille, K., and Dahm, T. Seismicity and velocity structure of the Southern Chilean subduction zone (between 37 ° and 39 ° S) revealed by the TIPTEQ local seismic network. *AGU Fall Meeting Abstracts*, pages D460+, December 2006.

[57] Hermann, J., Spandler, C., Hack, A., and Korsakov, A. V. Aqueous fluids and hydrous melts in high-pressure and ultra-high pressure rocks: Implications for element transfer in subduction zones. *Lithos*, 92:399–417, December 2006.

[58] Heubeck, C. and Mann, P. Geologic evaluation of plate kinematic models for the northern Caribbean plate boundary zone. *Tectonophysics*, 191:1–26, 1991.

[59] Hilairet, N., Reynard, B., Daniel, I., Wang, Y., Nishiyama, N., Petitgirard, S., and Merkel, S. Rheology of serpentines and mass transfer in subduction zones. *AGU Fall Meeting Abstracts*, pages G8+, December 2006.

[60] Hirn, A., Nicolich, R., Gallart, J., Laigle, M., and Cernobori, L. Roots of Etna volcano in faults of great earthquakes. *Earth and Planetary Science Letters*, 148:171–191, February 1997.

[61] Hirn, A., Singh, S., Charvis, P., Géli, L., Laigle, M., Lépine, J.-C., de Voogd, B., Saatcilar, R., Taymaz, T., Ozalaybey, S., Shimamura, H., Selvi, O., Karabulut, H., Murai, Y., Nishimura, Y., Yamada, A., Vigner, A., Bazin, S., Tan, O., Yolsal, S., Aktar, M., Galvé, A., Sapin, M., Marthelot, J.-M., Imren, C., Ergin, M., Tapirdamaz, C., Koçaoglu, A., Tarancioglu, A., Diaz, J., Verhille, J., Auffret, Y., Cetin, S., Oçakoglu, N., Karakoç, F., Klien, E., Ricolleau, A., Selvigen, V., Demirbag, E., Hakyemez, Y., and Sarikawak, K. Seismarmara 2001: A Marine Seismic Survey and Offshore-onshore Artificial Source and Natural Earthquakes In The Seismogenic Region of The Sea of Marmara. *EGS XXVII General Assembly, Nice, 21-26 April 2002, abstract #547*, 27:547–+, 2002.

[62] Hirn, Alfred and Laigle, Mireille. GEOPHYSICS: Silent Heralds of Megathrust Earthquakes? *Science*, 305(5692):1917–1918, 2004.

[63] Hirose, H., Kao, H., and Obara, K. Comparative Study of Nonvolcanic Tremor Locations in the Cascadia Subduction Zone Using two Different Methods. *AGU Fall Meeting Abstracts*, pages A1533+, December 2006.

[64] Holcombe, T. L. et al. *Caribbean marine geology: Ridges and basins of the plate interior.* 1990.

[65] Hu, Y. and Wang, K. Stable and Critical Coulomb Wedges: Stress Solution and Applications to Subduction Zones. *AGU Fall Meeting Abstracts*, pages B1639+, December 2006.

[66] Husen, S., Kissling, E., and Quintero, R. Tomographic evidence for a subducted seamount beneath the Gulf of Nicoya, Costa Rica: The cause of the 1990 Mw = 7.0 Gulf of Nicoya earthquake. *Geophysical Research Letters*, 29:79–1, April 2002.

[67] Insergueix-Filippi, D., Dupeyrat, L., Tric, E., and Menvielle, M. The influence of plate kinematics, convection intensity, and subduction geometry on the Earth's upper-mantle dynamics in the vicinity of a subduction zone. *Geophysical Journal International*, 138:275–284, July 1999.

[68] Ito, Y. and Obara, K. Detection of very-low-frequency earthquakes coincident with episodic tremors and slow slip events in the transition zone of the subducting plate interface. *AGU Fall Meeting Abstracts*, pages A1537+, December 2006.

[69] Ito, Y. and Obara, K. Very-low-frequency earthquakes within the accretionary prism and in the transition zone along the Nankai subduction zone. *AGU Fall Meeting Abstracts*, pages A8+, December 2006.

[70] Jordan, T. H. The present-day motions of the Caribbean plate. *Journal of Geophysical Research*, 80:4433–4439, November 1975.

[71] Kelley, K. A. and Hauri, E. H. Distribution of Water Across the Subduction Zone Mantle Wedge. *AGU Fall Meeting Abstracts*, pages G5+, December 2006.

[72] Kerrick, D. M. and Connolly, J. Thermodynamic Computation of Metamorphic Decarbonation for Marine Sediments Entering the Izu-Bonin-Mariana and Central America Subduction zones. *AGU Fall Meeting Abstracts*, pages B6+, December 2006.

[73] Kissling, E., Husen, S., and Haslinger, F. Model parametrization in seismic tomography: a choice of consequence for the solution quality. *Physics of the Earth and Planetary Interiors*, 123:89–101, April 2001.

[74] Kneller, E. A., van Keken, P. E., Katayama, I., and Karato, S. Stress, strain, and B-type olivine fabric in the fore-arc mantle: Sensitivity tests using high-resolution steady-state subduction zone models. *Journal of Geophysical Research (Solid Earth)*, 112:4406–+, April 2007.

[75] Kopp, H., Flueh, E. R., Papenberg, C., and Klaeschen, D. Seismic investigations of the O'Higgins Seamount Group and Juan Fernández Ridge: Aseismic ridge emplacement and lithosphere hydration. *Tectonics*, 23:2009–+, March 2004.

[76] Laigle, M., Hirn, A., Sachpazi, M., and Clément, C. Seismic Coupling and Structure of The Hellenic Subduction In The Ionian Islands Region. *EGS XXVII General Assembly, Nice, 21-26 April 2002, abstract #2519*, 27:2519–+, 2002.

[77] Laigle, M., Hirn, A., Sapin, M., Lépine, J.-C., Diaz, J., Gallart, J., and Nicolich, R. Mount Etna dense array local earthquake P and S tomography and implications for volcanic plumbing. *Journal of Geophysical Research*, 105:21633–21646, September 2000.

[78] Laigle, M., Roux, E., Sapin, M., Hirn, A., de Voogd, B., Charvis, P., Hello, Y., Murai, Y., Nishimura, Y., Shimamura, H., Galve, A., Lepine, J., Lebrun, J., Diaz, J., Gallart, J., Beauducel, F., and Viode, J. Elements of the Seismic Structure and Activity of the Lesser Antilles Subduction Zone (Guadeloupe and Martinique Islands) from the SISMANTILLES Seismic Survey. *AGU Fall Meeting Abstracts*, pages C580+, December 2005.

[79] Laigle, M., Sachpazi, M., and Hirn, A. Variation of seismic coupling with slab detachment and upper plate structure along the western Hellenic subduction zone. *Tectonophysics*, 391:85–95, October 2004.

[80] Lange, C., Haberland, C., Rietbrock, A., Bataille, K., and Dahm, T. Seismicity and Geometry of the Southern Chilean Subduction Zone Between 41.5 ° S and 43.5 ° S (Project TIPTEQ). *AGU Fall Meeting Abstracts*, pages D458+, December 2006.

[81] Lange, D., Rietbrock, A., Haberland, C., Bataille, K., Dahm, T., Tilmann, F., and Flüh, E. R. Seismicity and geometry of the south Chilean subduction zone (41.5 ° S-43.5 ° S): Implications for controlling parameters. *Geophysical Research Letters*, 34:6311–+, March 2007.

[82] Le Friant, A., Boudon, G., Deplus, C., and Villemant, B. Large-scale flank collapse events during the activity of Montagne Pelée, Martinique, Lesser Antilles. *Journal of Geophysical Research (Solid Earth)*, 108, January 2003.

[83] Lo, C., Hsu, S., and Chao, B. F. The Ryukyu subduction zone segmentation inferred from the GPS and earthquake-induced gravitational potential energy change. *AGU Fall Meeting Abstracts*, pages D1556+, December 2006.

[84] Long, H., Weidner, D., Li, L., Chen, J., and Wang, L. Investigation on Deformation of Olivine at Subduction Zone Conditions. *AGU Fall Meeting Abstracts*, pages B142+, December 2006.

[85] Loveless, J. P., Allmendinger, R. W., Pritchard, M. E., and González, G. A permanent record of subduction zone earthquake cycle deformation in the northern Chilean forearc. *AGU Fall Meeting Abstracts*, pages B421+, December 2006.

[86] Mann, P. et al. Actively evolving microplate formation by oblique collision and sideways motion along strike-slip faults: An example from the northeastern Caribbean plate margin. *Tectonophysics*, 246:1–69, 1995.

[87] Mascle, A. and Letouzey, A. Geological Map of the Caribbean. 1990.

[88] Matson, S. E., Rodriguez, H., Jansma, P. E., and Mattioli, G. S. GPS geodesy in the northern Lesser Antilles: implications for arc kinematics and subduction zone dynamics. *AGU Fall Meeting Abstracts*, pages B1307+, December 2002.

[89] McAdoo, D. C. Geoid anomalies in the vicinity of subduction zones. *Journal of Geophysical Research*, 86:6073–6090, July 1981.

[90] McNeill, L., Henstock, T., Tappin, D., and Curray, J. Forearc morphology and thrust vergence, Sunda subduction zone. *AGU Fall Meeting Abstracts*, pages A7+, December 2006.

[91] Mehl, L. Y., Barkman, J. E., and Baxter, E. F. Constraining the Rate of Water-Releasing Metamorphic Reactions in Subduction Zones. *AGU Fall Meeting Abstracts*, pages C519+, December 2006.

[92] Melbourne, T. I., Santillan, M. V., Szeliga, W., and Miller, M. GPS constraints on 34 slow slip events within the Cascadia subduction zone since 1997. *AGU Fall Meeting Abstracts*, pages G6+, December 2006.

[93] Minshull, T. A. and Charvis, P. Ocean island densities and models of lithospheric flexure. *Geophysical Journal International*, 145:731–739, June 2001.

[94] Montuori, C., Cimini, G. B., and Favali, P. Teleseismic tomography of the southern Tyrrhenian subduction zone: New results from seafloor and land recordings. *Journal of Geophysical Research (Solid Earth)*, 112:3311–+, March 2007.

[95] Mori, J. Observations and Mechanisms for Continuous Tremor and Low-Frequency Events in Subduction Zones. *AGU Fall Meeting Abstracts*, pages A5+, December 2006.

[96] Obara, K., Ito, Y., Sekine, S., Hirose, H., and Shiomi, K. Phenomenology of non-volcanic deep tremor, slow slip and the third slow earthquake in southwest Japan subduction zone. *AGU Fall Meeting Abstracts*, pages A1532+, December 2006.

[97] Okamoto, A., Kikuchi, T., and Tsuchiya, N. Mineral Growth Controlled By Aperture Of Fluid-filled Cracks In Subduction Zones: An Example From The Sanbagawa Belt, Japan. *AGU Fall Meeting Abstracts*, pages C1095+, December 2006.

[98] Orozco-Esquivel, T., Petrone, C. M., Ferrari, L., Tagami, T., and Manetti, P. Geochemical and isotopic variability in lavas from the eastern Trans-Mexican Volcanic Belt: Slab detachment in a subduction zone with varying dip. *Lithos*, 93:149–174, January 2007.

[99] Peterson, C., Christensen, D., McNutt, S., and Freymueller, J. Non-Volcanic Tremor in the Alaska/Aleutian Subduction Zone and its Relation to Slow-Slip Events. *AGU Fall Meeting Abstracts*, pages A1550+, December 2006.

[100] Pichavant, M., Martel, C., Bourdier, J.-L., and Scaillet, B. Physical conditions, structure, and dynamics of a zoned magma chamber: Mount Pelée (Martinique, Lesser Antilles Arc). *Journal of Geophysical Research (Solid Earth)*, 107:1–1, May 2002.

[101] Pratt, T. L. Do Episodic Tremor and Slip (ETS) Events Affect Seismicity in the Northern Cascadia Subduction Zone? *AGU Fall Meeting Abstracts*, pages A4+, December 2006.

[102] Pritchard, M. E., Norabuena, E. O., Ji, C., Boroschek, R., Comte, D., Simons, M., Dixon, T. H., and Rosen, P. A. Geodetic, teleseismic, and strong motion constraints on slip from recent southern Peru subduction zone earthquakes. *Journal of Geophysical Research (Solid Earth)*, 112:3307–+, March 2007.

[103] Ramachandran, K., Hyndman, R. D., and Brocher, T. M. Regional P wave velocity structure of the Northern Cascadia Subduction Zone. *Journal of Geophysical Research (Solid Earth)*, 111:12301–+, December 2006.

[104] Robson, G. R. An earthquake catalogue for the Eastern Caribbean 1530-1960 . *Bulletin of the Seismological Society of America*, 54:785–832, 1964.

[105] Rokosky, J. M., Schwartz, S. Y., and Obara, K. Characteristics of subduction zone tremor in SW Japan. *AGU Fall Meeting Abstracts*, pages A1699+, December 2006.

[106] Saffer, D. M. Pore pressure development and progressive dewatering in underthrust sediments at the Costa Rican subduction margin: Comparison with northern Barbados and Nankai. *Journal of Geophysical Research (Solid Earth)*, 108:9–1, May 2003.

[107] Salas-de La Cruz, M., Fischer, K. M., Forsyth, D. W., Abers, G. A., Strauch, W., Protti, M., and Gonzalez, V. Rayleigh Wave Tomography in the Nicaragua-Costa Rica Subduction Zone. *AGU Fall Meeting Abstracts*, pages C508+, December 2006.

[108] Sallarès, V. and Charvis, P. Crustal thickness constraints on the geodynamic evolution of the Galapagos Volcanic Province. *Earth and Planetary Science Letters*, 214:545–559, September 2003.

[109] Sallarès, V., Charvis, P., Flueh, E. R., and Bialas, J. Seismic structure of the Carnegie ridge and the nature of the Galápagos hotspot. *Geophysical Journal International*, 161:763–788, June 2005.

[110] Sanchez-Valle, C., Daniel, I., Martinez, I., Simionovici, A. S., Bass, J., and Reynard, B. Chemical composition and thermodynamical properties of high-pressure aqueous fluids in subduction zones from experiments in the diamond-anvil cell. *AGU Fall Meeting Abstracts*, pages D3+, December 2006.

[111] Sandoval, S., Kissling, E., and Ansorge, J. High-resolution body wave tomography beneath the SVEKALAPKO array - II. Anomalous upper mantle structure beneath the central Baltic Shield. *Geophysical Journal International*, 157:200–214, April 2004.

[112] Sandwell, D. and Smith, W. Global seafloor topography from dense satellite altimetry and sparse ship soundings (MGE). In Guyenne, T.-D. and Danesy, D., editors, *ESA SP-414: Third ERS Symposium on Space at the service of our Environment*, pages 1879–+, 1997.

[113] Savage, B. Subduction Zone Waveguides in Tonga-Fiji. *AGU Fall Meeting Abstracts*, pages C500+, December 2006.

[114] Scherwath, M., Contreras-Reyes, E., Tilmann, F., Grevemeyer, I., Flueh, E., and Weinrebe, W. Subduction of Young Oceanic Lithosphere in the Vicinity of the Chile Triple Junction - Little Influence of the Age of the Subducting Plate on the Overriding Plate. *AGU Fall Meeting Abstracts*, pages D461+, December 2006.

[115] Schultheiss, P. J. Pore pressures in marine sediments: An overview of measurement techniques and some geological and engineering applications. *Marine Geophysical Researches*, 12(1-2):153–168, 1989.

[116] Schulze, A., Micksch, U., Krawczyk, C. M., Ryberg, T., and Stiller, M. The Seismogenic Coupling Zone in Southern Central Chile, 38 ° S: A Reflection seismic image of the subduction zone (Project TIPTEQ). *AGU Fall Meeting Abstracts*, pages D456+, December 2006.

[117] Schwartz, S. Y. and Rokosky, J. M. A Global Review of Slow Slip Events and Seismic Tremor at Circum-Pacific Subduction Zones. *AGU Fall Meeting Abstracts*, pages A1+, December 2006.

[118] Screaton, E., Carson, B., Davis, E., and Becker, K. Permeability of a decollement zone: Results from a two-well experiment in the Barbados accretionary complex. *Journal of Geophysical Research*, 105:21403–21410, September 2000.

[119] Screaton, E. and Ge, S. Anomalously high porosities in the proto-decollement zone of the Barbados accretionary complex: Do they indicate overpressures? *Geophysical Research Letters*, 27:1993–1996, July 2000.

[120] Seward, A. M., Smith, E. C., and Henderson, M. Behind the Subduction Zone: Seismic Wave Speeds in the Upper Mantle Wedge Beneath the Central North Island, New Zealand. *AGU Fall Meeting Abstracts*, pages C507+, December 2006.

[121] Sharp, T. G., Diedrich, T., Dufrane, W., and Leinenweber, K. Subduction of hydrated lithosphere: small amounts of H2O greatly increase would eliminate metastable olivine in the transition zone. *AGU Fall Meeting Abstracts*, pages A7+, December 2006.

[122] Shi, Y. and Wang, C.-Y. Generation of high pore pressure in accretionary prisms: Inferences from the Barbados subduction complex. *Journal of Geophysical Research*, 93:8893–8910, August 1988.

[123] Smith, R. J., He, J., and Wang, K. Effects of 3-D Slab Geometry on Mantle Wedge Flow and Subduction Zone Thermal Regime. *AGU Fall Meeting Abstracts*, pages C520+, December 2006.

[124] Stein, S., Engeln, J. F., Wiens, D. A., Fujita, K., and Speed, R. C. Subduction seismicity and tectonics in the lesser Antilles arc. *Journal of Geophysical Research*, 87:8642–8664, October 1982.

[125] Stein, S. and Okal, E. A. How much, where and why? On the diversity of large earthquakes across subduction zones, including "silent" ones. *AGU Fall Meeting Abstracts*, pages F1+, December 2006.

[126] Styles, K. E., Stuart, G. W., Kendall, J., and Reyners, M. Seismic Anisotropy From Local Earthquakes in the Hikurangi Subduction Zone, North Island, New Zealand. *AGU Fall Meeting Abstracts*, pages C510+, December 2006.

[127] Sykes, L. R. and Ewing, M. The seismicity of the Caribbean region. *Journal of Geophysical Research*, 70:5065–5074, 1965.

[128] Tibi, R., Wiens, D. A., Shiobara, H., Sugioka, H., and Yuan, X. Detailed Image of the Subducting Plate and Upper mantle Seismic Discontinuities in the Mariana Subduction Zone. *AGU Fall Meeting Abstracts*, pages A391+, December 2006.

[129] Tilmann, F., Flueh, E., Planert, L., Reston, T., and Weinrebe, W. Microearthquake seismicity of the Mid-Atlantic Ridge at 5 ° S: A view of tectonic extension. *Journal of Geophysical Research (Solid Earth)*, 109:6102–+, June 2004.

[130] Ujiie, K., Yamaguchi, H., Sakaguchi, A., and Toh, S. Pseudotachylytes in an ancient accretionary complex and implications for melt lubrication during subduction zone earthquakes. *Journal of Structural Geology*, 29:599–613, April 2007.

[131] Špičák, A., Hanuš, V., and Vaněk, J. Earthquake occurrence along the Java trench in front of the onset of the Wadati-Benioff zone: Beginning of a new subduction cycle? *Tectonics*, 26:C1005+, February 2007.

[132] van Keken, P. E. The thermal state of subduction zones with implications for material transport into the deep mantle. *AGU Fall Meeting Abstracts*, pages B4+, December 2006.

[133] Waldhauser, F., Lippitsch, R., Kissling, E., and Ansorge, J. High-resolution teleseismic tomography of upper-mantle structure using an a priori three-dimensional crustal model. *Geophysical Journal International*, 150:403–414, August 2002.

[134] Wang, K. and Hu, Y. Role of Great Earthquakes in Building Thrust Wedges at Subduction Zones. *AGU Fall Meeting Abstracts*, pages G1+, December 2006.

[135] Warren, L. M., Silver, P. G., Langstaff, M. A., and Hughes, A. N. Deep Earthquake Mechanics and Deformation in the Tonga and Middle America Subduction Zones. *AGU Fall Meeting Abstracts*, pages A1+, December 2006.

[136] Weber, P. et al. GPS estimate of relative motion between the Caribbean and South American plates, and geologic implications for Trinidad and Venezuela. *Geology*, 29:75–78, 2001.

[137] Weldon, R. J., Burgette, R. J., and Schmidt, D. Along-Strike Variation in Locking on the Cascadia Subduction Zone, Oregon and Northern California. *AGU Fall Meeting Abstracts*, pages A1556+, December 2006.

[138] Westbrook, Bott, and Peacock. Geophysics-Lesser Antilles subduction zone in the vicinity of Barbados. *Nature Physical Science*, 244:118–+, August 1973.

[139] Westbrook, G. K. The structure of the crust and upper mantle in the region of Barbados and the Lesser-Antilles. *Geophysical Journal of the Royal Astronomical Society*, 43:201–242, 1975.

[140] Westbrook, G. K. The Barbados Ridge Complex: Tectonics of a mature forearc system. In: J.K. Leggett (Editor), Trench-forearc geology: sedimentary and tectonics on modern and active ancient plate margins. *Geological Society of London Special Publication*, 1982.

[141] White, W. M. and Dupré, B. Sediment subduction and magma genesis in the lesser antilles: Isotopic and trace element constraints. *Journal of Geophysical Research*, 91:5927–5942, May 1986.

[142] Wirth, R., Kaminsky, F., and Matsyuk, S. Nanoinclusions Of Phase Egg AlSiO3(OH), In Superdeep Diamonds From Juina (Brazil): Evidence For Subduction Of Crustal Components To Earth's Mantle Transition Zone. *AGU Fall Meeting Abstracts*, pages F4+, December 2006.

[143] Witter, R. C., Nelson, A. R., and Kelsey, H. M. Evidence for Seismogenic Segmentation of the Cascadia Subduction Zone From Coastal Paleoseismology. *AGU Fall Meeting Abstracts*, pages G3+, December 2006.

[144] Wu, F. T., Liang, W., and Lee, J. C. A Model for the Termination of the Ryukyu Subduction Zone against Taiwan - A Triple Junction of Collision, Subduction/Separation and Subduction Boundaries. *AGU Fall Meeting Abstracts*, pages B490+, December 2006.

[145] Zhao, Z., Moore, G. F., and Shipley, T. H. Deformation and dewatering of the subducting plate beneath the lower slope of the northern Barbados accretionary prism. *Journal of Geophysical Research*, 103:30431–30450, December 1998.

IFM-GEOMAR
Leibniz-Institut für Meereswissenschaften
an der Universität Kiel

IFM-GEOMAR Reports

No.	Title
1	RV Sonne Fahrtbericht / Cruise Report SO 176 & 179 MERAMEX I & II (Merapi Amphibious Experiment) 18.05.-01.06.04 & 16.09.-07.10.04. Ed. by Heidrun Kopp & Ernst R. Flueh, 2004, 206 pp. In English
2	RV Sonne Fahrtbericht / Cruise Report SO 181 TIPTEQ (from The Incoming Plate to mega Thrust EarthQuakes) 06.12.2004.-26.02.2005. Ed. by Ernst R. Flueh & Ingo Grevemeyer, 2005, 533 pp. In English
3	RV Poseidon Fahrtbericht / Cruise Report POS 316 Carbonate Mounds and Aphotic Corals in the NE-Atlantic 03.08.–17.08.2004. Ed. by Olaf Pfannkuche & Christine Utecht, 2005, 64 pp. In English
4	RV Sonne Fahrtbericht / Cruise Report SO 177 - (Sino-German Cooperative Project, South China Sea: Distribution, Formation and Effect of Methane & Gas Hydrate on the Environment) 02.06.-20.07.2004. Ed. by Erwin Suess, Yongyang Huang, Nengyou Wu, Xiqiu Han & Xin Su, 2005, to be published summer 2006. In English and Chinese
5	RV Sonne Fahrtbericht / Cruise Report SO 186 – GITEWS (German Indonesian Tsunami Early Warning System 28.10.-13.1.2005 & 15.11.-28.11.2005 & 07.01.-20.01.2006. Ed. by Ernst R. Flueh, Tilo Schoene & Wilhelm Weinrebe, 2006, 169 pp. In English
6	RV Sonne Fahrtbericht / Cruise Report SO 186 -3 – SeaCause II, 26.02.-16.03.2006. Ed. by Heidrun Kopp & Ernst R. Flueh, 2006, 174 pp. In English
7	RV Meteor, Fahrtbericht / Cruise Report M67/1 CHILE-MARGIN-SURVEY 20.02.-13.03.2006. Ed. by Wilhelm Weinrebe und Silke Schenk, 2006, 112 pp. In English
8	RV Sonne Fahrtbericht / Cruise Report SO 190 - SINDBAD (Seismic and Geoacoustic Investigations Along The Sunda-Banda Arc Transition) 10.11.2006 - 24.12.2006. Ed. by Heidrun Kopp & Ernst R. Flueh, 2006, 193 pp. In English
9	RV Sonne Fahrtbericht / Cruise Report SO 191 - New Vents "Puaretanga Hou" 11.01. - 23.03.2007. Ed. by Jörg Bialas, Jens Greinert, Peter Linke, Olaf Pfannkuche, 2007, xx pp. In English

10 FS ALKOR Fahrtbericht / Cruise Report AL 275 - Geobiological investigations and sampling of aphotic coral reef ecosystems in the NE-Skagerrak, 24.03. - 30.03.2006, Andres Rüggeberg & Armin Form, 39 pp. In English

11 FS Sonne / Fahrtbericht / Cruise Report SO 192-1: MANGO: Marine Geoscientific Investigations on the Input and Output of the Kermadec Subduction Zone, 24.03. - 22.04.2007, Ernst Flüh & Heidrun Kopp, xx pp. In English

Das Leibniz-Institut für Meereswissenschaften ist ein Institut der Wissenschaftsgemeinschaft Gottfried Wilhelm Leibniz (WGL)

The Leibniz-Institute of Marine Sciences is a member of the Leibniz Association (Wissenschaftsgemeinschaft Gottfried Wilhelm Leibniz).

Leibniz-Institut für Meereswissenschaften / Leibniz-Institute of Marine Sciences
IFM-GEOMAR
Dienstgebäude Westufer / West Shore Building
Düsternbrooker Weg 20
D-24105 Kiel
Germany

Leibniz-Institut für Meereswissenschaften / Leibniz-Institute of Marine Sciences
IFM-GEOMAR
Dienstgebäude Ostufer / East Shore Building
Wischhofstr. 1-3
D-24148 Kiel
Germany

Tel.: ++49 431 600-0
Fax: ++49 431 600-2805
www.ifm-geomar.de